Sede Amministrativa: Università degli Studi di Padova
Dipartimento di Biologia

SCUOLA DI DOTTORATO DI RICERCA IN : Bioscienze e Biotecnologie
INDIRIZZO: Biochimica e Biofisica
CICLO: XXVI

THE ROLE OF MITOCHONDRIAL DYSFUNCTION IN HUNTINGTON'S DISEASE PATHOGENESIS AND ITS RELATION WITH STRIATAL RHES PROTEIN

Direttore della Scuola : Ch.mo Prof. Giuseppe Zanotti
Coordinatore d'indirizzo: Ch.mo Prof. Fabio Di Lisa
Supervisore :Ch.mo Prof. Fabio Di Lisa

Dottorando : Marta Argenti

Index

Abbreviations

BDNF	brain derived neurotrophic factor
CRC	calcium retention capacity
CREB	cAMP response element binding protein
$\Delta\psi_m$	mitochondrial membrane potential
Drp1	dynamin related protein 1
ETC	electron transport chain
GFP	green fluorescent protein
HAP1	huntingtin associated protein 1
HIP	huntingtin interacting protein
HD	Huntington's disease
Htt	huntingtin
IMM	inner mitochondrial membrane
IT15	interesting transcript 15
mHtt	mutant huntingtin
Mfn	mitofusin
mTOR	mammalian target of rapamycin
NMDA	N-methyl-D-aspartate receptor
NOX	nicotinamide adenine dinucleotide phosphate oxidase
OMM	outer mitochondrial membrane
OXPHOS	oxidative phosphorilation
polyQ	polyglutamine
PGC-1α	peroxisome proliferator-activated receptor gamma coactivator 1 alpha
PTP	permeability transition pore
Opa1	optic atrophy 1
REST	repressor element-1 silencing transcription factor
ROS	reactive oxygen species
SDS	sodium dodecyl sulphate
SUMO	small ubiquitin-like modifier
UPS	ubiquitin-proteasome system
YAC128	yeast artificial chromosome 128

1. Summary

Huntington's disease (HD) in a fatal and hereditary neurodegenerative disorder. It is caused by a single mutation within the gene which codes for huntingtin protein (Htt). Mutant Htt (mHtt) bears an abnormally long polyglutamine expansion at its N-terminus that makes the protein cytotoxic and prone to aggregation. It is known that mHtt can negatively affect several different cell processes and mitochondrial function appears to be particularly injured. What is still under debate is whether mitochondrial dysfunction represents just an epiphenomenon of the cellular degeneration or it has an actual pathogenic role. To dissect this issue a wide analysis was performed of the mitochondrial function in multiple HD model, both cellular and animal.

We observed that mitochondria of striatal cells expressing mHtt maintain their basal respiration rate and membrane potential unaltered, even if mHtt causes an impairment of the electron transport chain. Moreover, the expression of N-terminal mHtt, that is known to reproduce a severe phenotype of the disease, increases cell death, but this does not seem to correlate with mitochondrial damage. In addition, starting from the presymptomatic phase, in HD mice brain mitochondria develop an enhanced resistance towards permeability transition induced by Ca^{2+}. This is presumably an adaptive change arisen to cope with mHtt-related stress.

These observations lead to hypothesize that mHtt *per se* does not affect mitochondria as a primary effect. It is rather likely that the mitochondrial impairment detected in some HD models comes after the alteration of other key cellular process.

Mitochondria dysfunction in HD has been further characterized by identifying the striatal protein Rhes as a relevant contributor of this phenotype. It has been previously demonstrated that Rhes increases mHtt cytotoxicity with a mechanism that has still to be fully understood. Here we showed that the coexpression of mHtt and Rhes leads to increased susceptibility to oxidative stress and loss of mitochondrial membrane potential. Conversely, the expression of the two proteins separately does not have any effect.

Sommario

La corea di Huntington (HD) è una malattia neurodegenerativa letale ed ereditaria. Essa si sviluppa in seguito ad una singola mutazione sul gene che codifica per la proteina huntingtina (Htt). La Htt mutata (mHtt) presenta all'N-terminale una coda poliglutamminica più lunga della forma *wild-type* e questo la rende prona all'aggregazione e citotossica. La mHtt può ostacolare la funzionalità cellulare a vari livelli e, in particolar modo, è stato dimostrato che l'espressione della mHtt si accompagna ad un'alterazione dell'attività mitocondriale. Nonostante il gran numero di studi sull'argomento non è ancora stato chiarito se questo danno sia la causa primaria della morte neuronale o semplicemente un effetto secondario dello stress indotto dalla mHtt.

Al fine di ottenere evidenze a sostegno dell'una o dell'altra ipotesi, è stata fatta un'analisi a largo raggio sulla funzionalità mitocondriale nell'*handling* del Ca^{2+} e nella respirazione in vari modelli di HD, sia cellulari sia animali. Si è osservato che nelle cellule striatali esprimenti mHtt i mitocondri mantengono inalterata la loro respirazione basale e il loro potenziale di membrana nonostante la mHtt indebolisca l'attività della catena di trasporto degli elettroni. L'espressione del solo N-terminale della mHtt, ossia la sua porzione più tossica, causa un aumento di morte cellulare che non sembra correlare con un danno a livello mitocondriale. Inoltre, fin da una fase presintomatica della malattia, i mitocondri isolati da cervello di topi HD si dimostrano più resistenti nei confronti dell'induzione della transizione di permeabilità, presumibilmente come forma di adattamento allo stress cellulare procurato dall'accumulo di mHtt.

Queste osservazioni portano ad ipotizzare che la mHtt di per sé non leda la funzionalità mitocondriale come effetto primario e che l'alterazione che si riscontra in alcuni modelli di HD sia, in effetti, una conseguenza del malfunzionamento di altri processi chiave nella cellula.

Un ulteriore passo avanti nella caratterizzazione della disfunzione mitocondriale nella HD è stato fatto identificando la proteina striatale Rhes come possibile corresponsabile, insieme alla mHtt, di questo fenotipo. In precedenza è stato visto che questa proteina aumenta la citotossicità della mHtt attraverso meccanismi ancora da definire. In questo studio è stato dimostrato che la co-espressione della mHtt con Rhes porta ad una perdita

di potenziale mitocondriale e ad aumentata suscettibilità allo stress ossidativo, laddove, invece, l'espressione delle due proteine singolarmente non sortisce alcun effetto.

2. Introduction

2.1 Huntington's disease

2.1.1 Genetic and clinical aspects

Huntington's disease in a fatal dominant inherited neurodegenerative disorder caused by a single mutation within the coding region of the IT15 (*interesting transcript 15*) gene. The IT15 gene is located on the short arm of chromosome 4 (4p16.3) and codes for a protein called huntingtin (Htt). The mutant gene has an increased number of cytosine-adenine-guanine (CAG) repeats at the 5'-end of exon 1 compared with the wild-type form (Fig. 1). The mutation gives rise to an elongated polyglutamine tract at the N-terminus of the Htt protein that is associated with protein aggregation and endows the protein with new toxic functions that are deleterious for brain cells.[1, 2]

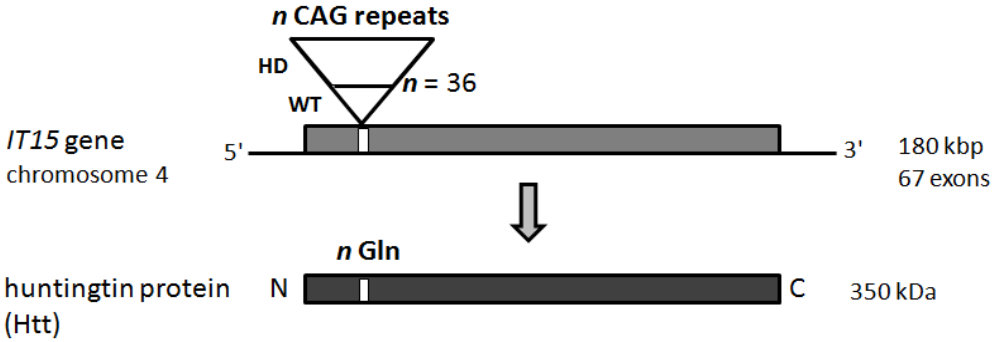

Fig. 1. Schematic representation of Htt protein and gene. In Huntington's disease an expansion beyond 36 of the CAG repeats at the 5'-end of exon 1 results in an abnormal elongation of the polyglutamine tail at the N-terminus of the protein.

Healthy individuals have typically less than 36 CAG repeats, 36-39 repeats indicate an incomplete penetrance of the disease,[3] while repeats of 40 or above result in HD with complete penetrance.

The CAG repeat length is a main determinant for HD onset, accounting for nearly 70% of the variability observed in the age at onset.[4] The number of CAG repeats varies considerably among patients: a repeat length around 40 is associated with adult onset of disease (between 35 and 50 years), whereas expansions of more than 60 repeats lead to a juvenile onset. Typically, a longer CAG repeat expansion correlates with an earlier onset, a more severe phenotype and more rapid progression of the disease.[5]

Prevalence of the mutation is 4–10 cases per 100,000 in populations of Western European descent, with many more at risk of having inherited the mutant gene without knowing it.

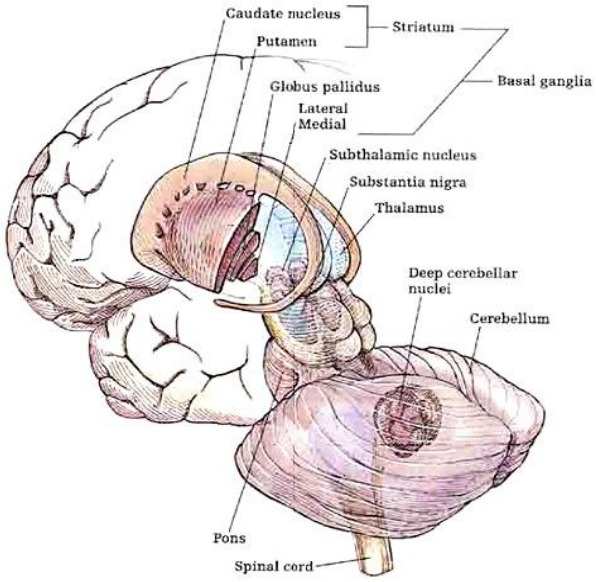

Fig. 2. Representation of the basal ganglia components and other relevant surrounding structures. Basal ganglia includes the striatum, the globus pallidus, the substantia nigra, the nucleus accumbens and the subthalamic nucleus. The striatum is the largest component of the basal ganglia and it is made of two distinct masses: caudate and putamen. About 96% of the striatal neurons are "medium spiny neurons". These are GABAergic neurons with small cell bodies and dendrites densely covered with dendritic spines, which receive synaptic input primarily from the cortex and thalamus. *From http:// www.epistemic-forms.com*

Over time, the consequence of carrying the HD mutation is a massive brain neurodegeneration characterized by the prevalent loss of medium spiny neurons in the striatum (caudate nucleus and putamen) of the basal ganglia (Fig. 2), which is primarily responsible for the typical HD symptoms.[6] The most common grading system to evaluate the severity of HD progression refers to the extent of striatal degeneration in *post mortem* tissue and classifies HD cases into five different severity grades (0–4).[7]

Although the striatum is the most profoundly affected region in HD, it is now well established that a more widespread degeneration occurs in the brain and can involve

also cerebral cortex (particularly layers III, V, and VI), globus pallidus, thalamus, hypothalamus, subthalamic nucleus, substantia nigra and cerebellum (Fig. 3).[8, 9]

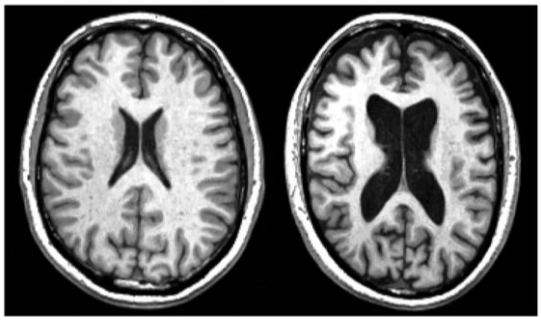

Fig. 3. Brain magnetic resonance imaging of a healthy individual (left) and a patient with HD (right). Loss of striatal mass is apparent early in HD, as the disease progress a severe atrophy affects also other brain regions. *From http://kobiljak.msu.edu*

The clinical phenotype of HD is characterized by progressive motor impairments, cognitive deterioration, personality changes and susceptibility to severe mental disorder. The disease progression is slow and HD mutation leads to death after ten to twenty-five years from first symptom appearance.

In the early stages, HD is typically associated with progressive emotional, psychiatric, and cognitive disturbances.[10] Commonly reported symptoms in HD include progressive weight loss, alterations in sexual behaviour and in the wake-sleep cycle that appear very early in the course of the disease and may partly be determined by hypothalamic dysfunction.[11] In the later stages, HD patients show motor deficiencies, progressive dementia, or gradual impairment of the mental processes involved in comprehension, reasoning, judgment, and memory.[12, 13] Due to increasingly severe dementia and progressive motor dysfunction, patients with advanced HD may become unable to walk, have poor dietary intake, eventually cease to talk, and become unable to care for themselves, therefore potentially requiring long-term institutional care. Life-threatening complications may result from injuries related to serious falls, poor nutrition, infection, choking, and inflammation. Most HD patients eventually die of cardiac failure or aspiration pneumonia because of swallowing difficulties.[10]

Currently, HD therapy can only limit chorea, that is the involuntary and irregular movements of the limbs that characterized this disorder, and battle the mood altering aspects of HD, since no disease modifying treatment is available.

The expansion of CAG tracts encoding polyglutamine stretches is the cause of other nine human neurodegenerative diseases: besides HD, the others are dentatorubral-

pallidoluysian atrophy, spinobulbar muscular atrophy, and spinocerebellar ataxia types 1, 2, 3, 6 and 7. These disorders are all characterized by abnormal polyQ expansion of a specific protein and loss of a specific type of neurons.[14]

2.1.2 Wild-type huntingtin

Htt is a large protein with a mass of 347 kDa that is made up of 3144 amino acids. It is ubiquitously expressed in humans and rodents, with highest concentrations in the neurons of the central nervous system.[15, 16] Htt is particularly enriched in cortical pyramidal neurons in layers III and V that project to the striatal neurons.[17]

Within the cell, Htt is mainly found in the cytoplasm but it can associate with the nucleus and a variety of organelles, including endoplasmic reticulum, Golgi complex, and mitochondrion.[18, 19] It has also been found within neurites and at synapses, where it can associate with various vesicular structures such as clathrin-coated vesicles, endosomes, caveolae, and microtubules.[19, 20] This widespread subcellular localization does not facilitate the definition of Htt physiological function.

An evident feature of the Htt protein is the polyQ at its N-terminus. In higher vertebrates, and specifically in mammals, the polyQ region is followed by a polyproline (polyP) stretch (Fig. 4). It has been suggested that the polyP region could have a role in mediating Htt interaction with other proteins and also in stabilizing the polyQ tract by keeping it soluble.

Htt is additionally enriched in the so-called HEAT repeat: a sequence of ~40 amino acids named after the first four proteins in which it was discovered: *H*untingtin, *E*longation factor 3, a subunit of protein phosphatase 2*A* and the lipid kinase *T*OR. Although the exact function of HEAT repeats is currently unclear, it has been proposed that these domains mediate protein-protein interaction. The identification of 37 putative HEAT repeats in Htt suggests that the normal function of Htt may involve some of these protein-protein interactions, pointing to the possible role of Htt as a scaffold protein.[21]

By using yeast two-hybrid screenings, affinity pull-down assays, western blotting, and immunoprecipitation, nearly 50 proteins able to directly interact with Htt or its fragments have actually been described.[22] These Htt interactors are involved in gene expression, intracellular transport, intracellular signaling and metabolism.[22, 23]

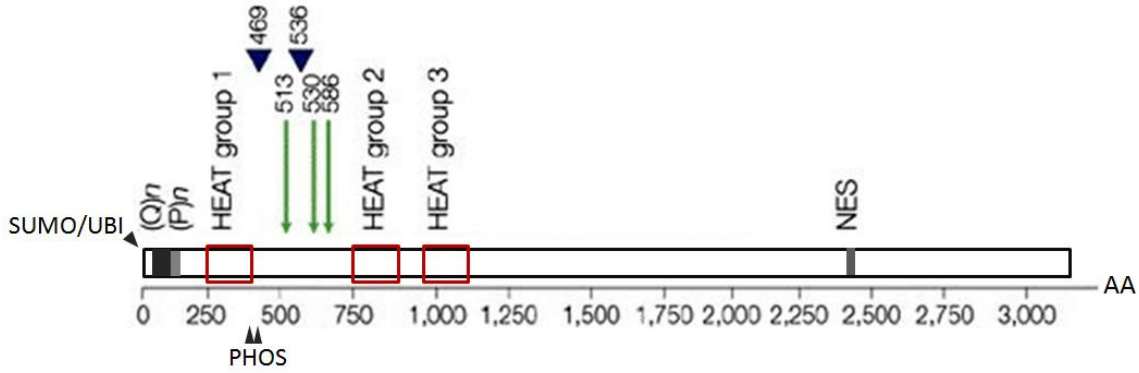

Fig. 4. Schematic diagram of Htt amino acid sequence. (Q)n indicates the polyglutamine tract, which is followed by the polyproline sequence, (P)n, and the red squares indicate the three main clusters of HEAT repeats. The green arrows indicate the caspase cleavage sites and their amino acid positions, and the blue arrowheads the calpain cleavage sites and their amino acid position. NES is the nuclear export signal. The black arrows indicate post-translational modifications: ubiquitination (UBI) and/or sumoylation (SUMO) at the first 17 amino acids, and phosphorylation (PHOS) at serine 421 and serine 434.

Determining the physiological function of wild-type Htt remains elusive, although several molecular pathways have been identified in which Htt plays a key role.

For example, Htt function in transcription is widely documented.[23] Htt can regulate transcription by shuttling transcription factors between the nucleus and the cytoplasm and by interacting with spliceosome-related proteins.[24] Moreover, Htt binds to RE1-Silencing Transcription factor (REST, also known as Neuron Restrictive Silencer Factor) and therefore sequesters it in the cytoplasm.[25] Htt activates transcription by keeping REST in the cytoplasm, away from its nuclear target: the neuron restrictive silencer element, which is a consensus sequence found in genes such as the that encoding brain derived neurotrophic factor (BDNF). BDNF has been proved to be particularly important for the survival of striatal neurons and for the activity of the cortico-striatal synapses.[26]

Evidence is growing to suggest that Htt is also involved in trafficking. Htt interacts with many proteins that regulate intracellular transport or endocytosis, such as Htt-associated protein 1 (HAP1), Htt-interacting protein 1 and 14 (HIP1 and HIP14), HIP1-related protein, protein kinase C and casein kinase substrate in neurons-1.[27, 28] Htt influences both anterograde and retrograde transport in the dendritic and axonal processes by binding with HAP1 and subsequently interacting with the molecular motors dynein/dynactin and kinesin.[29, 30] Through this interaction Htt promotes the transport of BDNF along microtubules. Indeed, a higher or lower Htt concentration in cells respectively increases or decreases intracellular transport of BDNF.[31]

In vitro and *in vivo* studies have shown that Htt has an anti-apoptotic effect. It has been observed that Htt prevents the activation of caspase-8 by interacting with HIP1 and hampering its association with HIP1-protein-interactor.[32] In fact, the complex formed by HIP1 and HIP1-protein-interactor induces caspase 8-mediated apoptosis in the cell. In addition, Htt blocks the formation of a functional apoptosome complex and the consequent activation of caspase-3 and caspase-9.[33, 34]

Studies in Htt knock-out mice have shown that Htt is required for normal embryonic development and neurogenesis: mice lacking Htt die at embryonic day 7.5.[35] Htt is also fundamental in adult life, as the inactivation of its gene in the brain of adult mouse leads to neurodegeneration.[36] Furthermore, wild-type Htt protects against cell death induced by mutant Htt *in vivo* and against neurodegeneration induced by ischaemia or NMDA receptor activation.[37]

Htt contains well-characterized consensus cleavage sites for proteolytic enzymes that cut the protein around the 500th amino acid residue and generate a wide range of fragments. Caspases, calpain, and aspartyl proteases are all involved in this process. Htt is cleaved by caspase-3 and caspase-7 at amino acids 513 and 552, caspase-6 at amino acid 586, and caspase-2 at amino acid 552.[38] Two specific calpain cleavage sites have been identified in Htt at residues 469 and 536.[39]

Htt can undergo several types of posttranslational modifications. It is ubiquitinated at the N-terminal lysines K6, K9 and K15 and thus targeted to the proteasome.[40] When an expanded polyQ stretch is present, this process is impaired causing proteosomal dysfunction.

Htt can be phosphorylated at serine-13, -16, -421, -434, -1181 and -1201. It is known that phosphorylation can influence Htt susceptibility to clearance by the proteasome or cleavage by proteases,[41] but it is still not clear how phosphorylation can regulate Htt physiological activity. Importantly, phosphorylation of mutant Htt modulates its toxicity and aggregate formation[42] suggesting that targeting serine residues may represent a potential therapeutic strategy for HD.

Htt is SUMOylated at the first 17 amino acids and SUMOylation modulates its subcellular localization, activity and stability.[43, 44]

Finally, Htt is palmitoylated,[45] as other proteins involved in vesicle trafficking, and acetylated at lysine-444.[46] Acetylation has been deeply studied in the case of mHtt as this modification facilitates mHtt engulfment by autophagosomes and this significantly improves its clearance and reverses mHtt toxic effects.[46]

2.1.3 Mechanisms of neurodegeneration

The exact molecular mechanism whereby mutation in Htt causes the observed striatal neurodegeneration, despite a ubiquitous expression, is still elusive. This mechanism is likely multifactorial, highly complex and may imply a coexistence of both loss-of-function and gain-of-function effects.
Indeed, mutant Htt is known to negatively affect several different aspects of cell life, such as transcription, ubiquitin-proteasome system, autophagy, calcium homeostasis, vesicular trafficking and mitochondrial function (Fig. 5). In addition, the mutation may also hinder the Htt protein from exerting its normal molecular activities that are crucial for the functioning and viability of neurons in general and striatal neurons in particular.

Aggregation and proteolysis. Mutant Htt is highly prone to aggregation. The formation of cytoplasmic aggregates and nuclear inclusions throughout the brain is one of the most striking hallmarks of HD.[47] Mutant Htt aggregates are made of highly ordered amyloid fibers with high β-sheet content and low detergent solubility. These inclusions can sequester several other proteins, including factors important for transcription and protein quality control, suggesting that their presence is deleterious to cell function and contributes to a complex loss of function phenotype. Several lines of evidence identify small oligomeric forms as the most toxic species and propose that the formation of large inclusions of mHtt might be a protective strategy as mHtt is held into a less pervasive structure.[48, 49] However, the role of aggregates in HD is still a matter of debate, especially because a precise correlation between aggregation level of mHtt and neuronal death has not been demonstrated yet.
As described above, Htt is susceptible to proteolysis by a number of proteases (cf. paragraph 2.1.2). Proteolytic fragments including the N-terminal part of the protein are detectable in brains of HD patients and HD mice before the loss of neurons in the striatum. Blocking mHtt cleavage by site-directed mutagenesis or by pharmacological approaches reduces cytotoxicity and slows down disease progression.[50] Moreover, when N-terminal mHtt fragments are overexpressed in cell or animal models, they reproduce the most severe traits of the full-length mHtt toxicity.[51] These evidences strongly suggest that proteolytic cleavage of the aberrant protein is a key step step in the development of HD and that N-terminal fragments are probably the major responsible of cell damage.

Transcriptional dysregulation. Alteration of gene transcription is certainly an important aspect of HD pathogenesis.[52] In fact, investigations based on DNA microarray technology showed a lot of gene expression changes in HD models and human *post mortem* brain tissue. Cell culture and biochemical studies indicated that mHtt can interfere with gene transcription.[53, 54] Several molecular mediators have been proposed, including cAMP response element binding protein (CREB),[55] nuclear receptor corepressor, SP1 transcription factor, basal transcription factors, and REST elements. Direct mHtt interaction with DNA might also play a part.[56] Mutant Htt interaction with CREB transcription factor can lead to reduced expression of the essential neurotrophic factor BDNF,[57] mitochondrial OXPHOS proteins (e.g. Cox-IV and cytochrome *c*) and PGC-1α,[54] that is a transcriptional co-activator regulating mitochondrial biogenesis and oxidative function.

Excitotoxicity and calcium dyshomeostasis. The excessive stimulation of excitatory amino acid receptors, especially of NMDA receptors, is defined as excitotoxicity. This has long been regarded as a non-cell autonomous mechanism with a role in pathogenesis of Huntington's disease.[58] The excessive stimulation of NMDA glutamate receptors may be due to increased glutamate release from cortical afferents and/or reduced uptake of glutamate by glia. Moreover, hypersensitivity of postsynaptic glutamate receptors on striatal projection neurons may also contribute to pathogenesis.[59] Excitotoxicity results in the dysfunction of neuronal interaction and circuitries at the corticostriatal synapse. In addition, the rise in cytosolic Ca^{2+} concentration can potentially bring to ROS overproduction and abnormal activation of several Ca^{2+}-dependent enzymes. The cell damage derived from cytosolic [Ca^{2+}] rise can be amplified by the defective buffering capacity of mHtt expressing cells, which is largely documented.[60] In some HD models it was observed that mHtt reduces the sensitivity of the mitochondrial permeability transition pore (PTP) to Ca^{2+}-induced opening with consequent release of Ca^{2+} from the matrix.[61] Moreover, mHtt binds to the inositol 1,4,5-triphosphate receptor 1 on the endoplasmic reticulum stimulating Ca^{2+} release.[62] This causes a further increase in cytosolic [Ca^{2+}] that is likely responsible for the general dysregulation of Ca^{2+}-homeostasis and Ca^{2+}-dependent signaling pathways observed in experimental HD models.

***Clearance systems*.** As in many neurodegenerative diseases associated with accumulation of misfolded proteins, also in HD a dysfunction in clearance systems takes place. Misfolded proteins can be cleared by both autophagy and ubiquitin-proteosome machinery. Mutant Htt can interfere with target recognition and compromise autophagic clearance causing a lower engulfment of cytosolic macromolecules and damaged organelles.[63] Pharmacological activation of mammalian target of rapamycin (mTOR)-dependent autophagy with rapamycin attenuates toxic effects of mHtt in fly and mouse model of HD.[64] The ubiquitin-proteosome system (UPS) has been an important topic of research in HD since mHtt aggregates were first observed to be ubiquitin-tagged, suggesting a failure in their degradation by UPS.[65] An accumulation of ubiquitin-positive proteins occurs in brain tissue from HD patients and HD mice.[66] The disruption of UPS likely arises because the proteostasis is impaired by mHtt. The lower activity of UPS in turn leads to increased level of improperly folded proteins and, as a consequence, the great amount of accumulated polyubiquitylated proteins overloads the proteasome preventing it from working efficiently. Inhibition of clearance systems amplifies mHtt own toxicity as it causes the accumulation of defective organelles and proteins different from Htt but potentially harmful.

***Vesicular trafficking*.** Wild-type Htt was found to be part of the motor complex that drives anterograde and retrograde transport of vesicles and organelles along the microtubules. Many evidences suggest that this motor complex is altered in HD. In particular, increased binding of mHtt to HAP1 was found to reduce the association between HAP1/dynactin and microtubules altering the mechanism of retrograde transport.[31] On the other hand, anterograde vesicular transport, particularly important for BDNF delivery to striatal cells, appears to be altered because of a defect in HAP1/Htt/kinesin complex formation. It has been also proposed that dysfunction in vesicular trafficking occurs because mHtt aggregates bind to cargoes impairing their movement or physically block their movement along the axons.[67] Finally, it is possible that mHtt aggregates impair vesicular trafficking because they recruit motor proteins, thus reducing the soluble pool of motor proteins required for transport.[68]

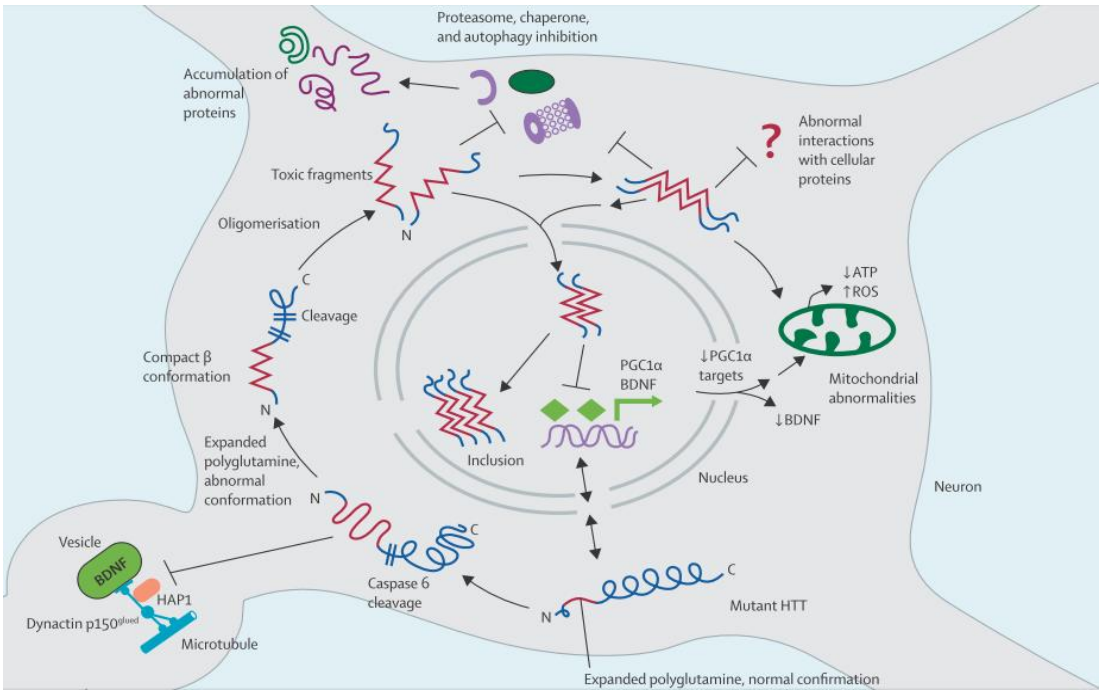

Fig. 5. Postulated intracellular pathogenesis of Huntington's disease. Mutant Htt with an expanded polyglutamine repeat undergoes a conformational change and interferes with cellular trafficking, especially of BDNF. Mutant Htt is cleaved at several points to generate toxic fragments with abnormal compact β conformation. Pathogenic species can be monomeric or, more likely, form small oligomers. Toxic effects in the cytoplasm include inhibition of chaperones, proteasomes, and autophagy. There may be direct interactions between mutant Htt and mitochondria. Mutant Htt inclusion bodies are found in the nucleus and in cytoplasmic regions. A major action of mutant Htt is interference with gene transcription leading to decreased transcription of BDNF and PGC1α. *From Ross et al., Lancet Neurol 2011; 10: 83–98.*

2.2 Mitochondrial dysfunction in Huntington's disease

Many lines of evidence suggest that mitochondrial dysfunctions play a central role in HD.[69] Mitochondria are key regulators of cell death, a main feature in neurodegeneration. Neurons are much sensitive to mitochondrial defects as they are characterized by particularly high energy demands. In fact, neurons have to fulfil expensive physiological functions like the release and re-uptake of neurotransmitters at synapses, a variable plasma membrane potential, and the trafficking of vesicles and organelles along extended processes. Moreover, they rely mainly on mitochondria as source of ATP production and do not switch to glycolysis when oxidative phosphorylation is impaired.[70] Several mitochondrial defects are documented in HD studies and a wide range of pathogenic mechanisms has been proposed, ranging from direct mHtt-mitochondria association[71, 72] to indirect transcriptional dysregulation

affecting mitochondrial composition (cf. paragraph 2.1.3).[73, 74] On the other hand, it has been for long debated whether mitochondrial dysfunction is just one of the consequences of the cellular degeneration or it has a causative pathogenic role. This doubt derived also from the fact that many hereditary and sporadic neurodegenerative disorders with different clinical phenotype and pathogenesis share similar mitochondrial alterations, suggesting that the mitochondrial contribution may be an aspecific feature of the disease progression. To address this issue in the context of HD, an extensive research has been dedicated to characterize the mechanisms whereby mHtt can affect mitochondrial function, in order to identify new potential therapeutic targets to modulate the progression of the disorder. The following paragraph reports a short overview of the main mitochondrial defects documented in HD.

***Energy metabolism and respiratory chain*.** In the cerebral cortex and basal ganglia of HD patients, increased production of lactate was observed,[75] suggestive of an elevated glycolytic rate. Moreover, positron emission tomography (PET) gave strong evidence for altered glucose metabolism in the brain of HD patients, especially in the basal ganglia, from the early stages of the disease.[76, 77] These alterations can possibly be due to mitochondrial impairment. ATP depletion was demonstrated in brain of an HD mouse model.[78] Furthermore, by means of ^{1}H-magnetic resonance spectroscopy, the basal ganglia and thalamus of symptomatic HD patients were shown to have low concentration of N-acetylaspartate, a molecule abundant in neurons, whose production depend on and is often regarded to reflect mitochondrial metabolic activity.[75, 79] A few studies have investigated whether defects in mitochondrial respiration contribute to the observed bioenergetic alterations. Severe reduction in the activity of complex II/III and milder reduction of complex IV were found in *post mortem* samples of caudate/putamen in HD patients.[80] No changes were observed in pre-symptomatic patients.[81] Lower activity of other enzymes involved in oxidative metabolism in the striatum was also reported. In particular, massive loss of aconitase and pyruvate dehydrogenase activity has been found in the caudate and putamen.[58, 82] However, these defects were observed in symptomatic patients with caudate/putamen atrophy. Since no significant deficiency of respiratory chain complexes has been documented in presymptomatic patients or in HD model mice expressing full-length mHtt, a causal relationship between cell injury and mitochondria dysfunction can not be established and it has been inferred that respiratory chain defects are likely a secondary feature in HD pathogenesis.

***Oxidative stress*.** Increased ROS production could be one of the causes of impaired respiratory chain. Evidence of enhanced oxidative stress in HD brains includes an increase in accumulation of lipofuscin, a product of unsaturated fatty acid peroxidation, that is more pronounced in vulnerable striatal neurons.[83] Oxidative modification of proteins (protein carbonyls) and lipids (malondialdehyde and 4-hydroxynonenal) are also increased in HD brain and in animal models,[83] and increased malondialdehyde is observed in blood.[84] Moreover, an increase in oxidative defense mechanisms, including mitochondrial and cytoplasmic superoxide dismutase, have been found in HD patient brains[85] and transgenic animals.[86]

Oxidative damage can contribute to neuronal loss in HD. However, it is not clear whether oxidative stress is a determining factor or, rather, a late event in the disease pathogenesis and even the origin of increased ROS has not been identified conclusively. Mitochondrial respiratory chain is a major source of ROS and defects of its complexes may cause ROS overproduction. Consistently, complex II inhibition models of HD display evidence of oxidative stress.[87]

Another trigger of mitochondrial ROS production has been proved to be Ca^{2+} dyshomeostasis. Wang and colleagues showed that higher level of mitochondrial matrix Ca^{2+} loading provokes elevated superoxide generation by mitochondria in HD neurons.[88] This in turn leads to higher level of mitochondrial DNA damage impinging on mitochondria function.

Nicotinamide adenine dinucleotide phosphate oxidase (NOX) has recently been identified as a key non-mitochondrial contributor of oxidative stress in HD.[89] NOX activity was found increased in human HD *post mortem* cortex and striatum and also in striatum of presymptomatic individuals.

***Calcium handling*.** Initial studies with isolated mouse brain mitochondria showed that those isolated from HD mice are characterized by higher Ca^{2+} vulnerability with respect to wild-type mitochondria. Vulnerability was proportional to mHtt levels and it was proposed to result from deleterious mHtt interaction with mitochondria membranes.[71] However, subsequent studies with brain mitochondria, isolated from diverse HD mice, revealed either no difference or decreased Ca^{2+} buffering capacity, indicating a higher susceptibility to Ca^{2+} loads.[90, 91] These opposite results with isolated mitochondria may be determined by different methodological approaches.[91, 92] Results may also be

influenced by the mixed composition of mitochondria suspensions as they can include different percentages of synaptic or non-synaptic and neuronal or glial mitochondria.[93]
Deficits in mitochondrial-dependent Ca^{2+} handling has been identified also in intact HD striatal neurons. In this model mHtt causes a delayed recovery to basal Ca^{2+} levels following NMDA receptor activation.[94] Thus, it has been proposed that, in HD pathogenesis, mitochondria could be downstream targets of abnormal NMDA receptor iperactivity.
HD literature provides many conflicting findings about the role of mitochondria in Ca^{2+} homeostasis so that it is still an unresolved issue. This emphasizes the need for a comprehensive study that analyzes multiple models with different methodological approaches. Such a study would allow to exclude that the obtained results are influenced by a specific experimental set-up. At the same time, it would be useful to investigate in parallel both the direct (Ca^{2+} uptake) and the indirect mitochondrial involvement in Ca^{2+} homeostasis (OXPHOS that fuel ATP-dependent non-mitochondrial Ca^{2+} handling mechanisms, e.g. Ca^{2+} endoplasmic reticulum pumps).

Motility and morphology. Although research on mitochondrial dysfunction has predominantly focused on changes in bioenergetics and Ca^{2+} handling, recently also alterations in mitochondrial dynamics has been investigated. Mitochondria are highly dynamic organelles organized in a network whose morphology is determined by continuous fusion and fission events precisely regulated by pro-fission (cytosolic Drp1 and its mitochondrial receptor Fis1) and pro-fusion (Opa1 in the IMM and Mfn1 and 2 in the OMM) proteins. Mutant Htt expression induces mitochondrial fragmentation in several HD models[95] making cells more sensitive to oxidative stress[96] and apoptotic stimuli.[95] Furthermore, it has been shown that mitochondrial fragmentation could be ameliorated by overexpressing a dominant negative version of the pro-fission Drp1 or the pro-fusion Mfn2.[97] Besides fragmentation, expression of polyQ expansion fragments also leads to disruption of cristae. This mitochondria remodelling seems to be crucial for their hypersensitivity to apoptosis.[95] Mitochondrial fragmentation in HD has been proposed to be due to an increased basal activity of the phosphatase calcineurin which, in turn, stimulates the pro-fission activity of Drp1.[95] Alternatively, mHtt can abnormally interact with Drp1 increasing its enzymatic activity.[98] Inhibition of Drp1 has very recently proved to diminish mitochondrial dysfunction, motor deficits and mortality in HD transgenic mice.[99]

Mitochondria, as well as other organelles like lysosomes, peroxisomes and ER, are actively transported along microtubules towards the cell regions where their function is required. In neurons, long-range movements on cytoskeletal elements are essential to transport the organelles along dendritic and axonal cell processes. Mutant Htt aggregates might physically block mitochondrial movement in neurons[67] or may also impair movement indirectly, namely by precipitating trafficking machinery proteins and wild-type Htt, which is needed for efficient axonal trafficking.[100] However, while in cortical neurons mitochondrial trafficking was reduced specifically where there are mHtt aggregates,[67] in striatal neurons mitochondrial trafficking was slower even in regions without mHtt aggregates.[101] This suggests that a mechanism responsible for the high vulnerability of striatal neurons to mHtt could imply the impairment of mitochondria trafficking. Interestingly, a reduced mitochondrial trafficking in wild-type striatal neurons with respect to cortical neurons was observed,[102] supporting the hypothesis that striatal mitochondria are significantly more vulnerable to trafficking impairments.

2.3 Rhes protein

Several *in vitro* e *in vivo* studies pointed out that Rhes, a small striatal G protein, could account for striatal specificity of HD neurodegeneration. Indeed, Rhes mediates mHtt cytotoxicity and is required to observe severe disease phenotype in HD mice. The reasons of the harmful consequences of mHtt-Rhes coexistence have not been completely explained yet.

2.3.1 Features and physiological role

Rhes is a 266 amino acid protein that was discovered during a screen for mRNAs predominantly expressed in rodent striatum.[103] Because of its homology with Ras proteins, it was named as *R*as *H*omolog *E*nriched in *S*triatum, or Rhes. Like Ras family proteins, Rhes contains GTP binding and effector domains and a CAAX box that can be farnesylated and mediates membrane localization. However, in addition, Rhes shares with the protein Dexras1 a C-terminal extension (95 amino acids in Rhes) that defines a new subgroup of Ras family proteins.[104]

Although Rhes mRNA is predominantly localized to brain, some other tissues show expression, like, for example, thyroid gland and pancreatic islets.[105] Moreover, RT-PCR studies indicated low expression in kidney, lung, heart, and testis.[106] Within brain, Rhes mRNA is preferentially expressed in striatum but it is also found in layers 2/3 and 5 of cerebral cortex, piriform cortex, olfactory tubercle and bulb, subiculum, hippocampus, anterior thalamic nucleus and cerebellum.[107]

The physiological role of Rhes protein is not completely defined, but it is clear that Rhes interacts with multiple proteins to affect striatal function at multiple levels.

Early studies focused on a role for Rhes in signaling by striatal G protein-coupled receptors. In cultured cell, Rhes was shown to inhibit signaling through G_s-coupled beta-adrenergic and dopamine D1 receptors,[108] as well as G_i-mediated signaling by muscarinic receptors.[109] $Rhes^{-/-}$mice display up-regulated $G_{s/olf}$-mediated signaling, indicated by increased phosphorylation of the target glutamate receptor 1 at the PKA site, suggesting that Rhes normally inhibits this pathway.[110] More recently, Rhes has been shown to bind to and activate mTOR increasing phosphorylation of targets of both mTOR complex 1 and 2.[111] mTOR is a key regulator of cell growth and survival and it regulates autophagy and protein synthesis in response to cellular nutrient, oxygen and energy levels.[112] Rhes appear to be the primary activator of mTOR in the striatum and, indeed, in $Rhes^{-/-}$mice mTOR signaling is reduced more than 70%.

Rhes is also involved in processes that are upstream of mTOR. In fact, it interacts with the regulatory subunit of PI3K upon growth factor treatment and it binds to Akt to enhance its phosphorylation.[113] Finally, Rhes protein can behave as a E3 SUMO-ligase catalyzing SUMOylation of several striatal proteins and promoting 'cross-SUMOylation' of E1- and E2-SUMO enzymes.[114]

Rhes expression is regulated by tyroid hormones during postnatal period. Rhes level is low during embryonic life and in early postnatal phases, becomes higher at postnatal days 15-30 and decreases during adulthood.[104] Rhes mRNA levels are influenced also by dopamine and, notably, striatum is particularly enriched in dopamine receptors. Removal of dopamine inputs to the striatum makes postsynaptic dopamine receptors supersensitive to dopamine and results in a decrease in Rhes mRNA expression. It is possible that these two events are correlated and it has been hypothesized that Rhes may play a role in determining normal dopamine receptor sensitivity.[115]

Mice with genetic deletion of Rhes are viable and do not display a distinctive phenotype. They weight slightly less than wild-type mice and show modest behavioural

abnormalities with increase in anxiety and motor coordination defects, but no memory or learning disruption.[106]

2.3.2 Rhes in Huntington's disease

In HD, the selective degeneration of the striatum is enigmatic since Htt protein is expressed not only in the whole brain, but also throughout the entire body. Although some degeneration of cerebral cortex was observed in the late stages of the disease, this is less severe than the striatal damage and may occur after the striatum atrophy. What has still to be understood is what is so striatum-specific that causes its selective vulnerability in HD. The striatal localization of Rhes pointed to this protein as a unique candidate, and, indeed, in a landmark paper in 2009, Subramaniam and colleagues described a role for Rhes in selective striatal degeneration in HD.[116] Rhes was shown to bind to wild-type Htt and, more tightly, to mHtt. On the other hand, Rhes did not bind to ataxin, the polyQ repeat protein responsible for spinocerebellar ataxia. Importantly, Rhes expression significantly increase mHtt cytotoxicity in HEK293 cells, immortalized striatal precursors and also primary striatal neurons.[117] Consistently, Rhes deletion is neuroprotective in the 3-nitropropionic acid model of HD,[118] $HD^{+}/Rhes^{-/-}$ mice showed remarkably delayed expression of HD-like symptoms[119] and Rhes deletion through RNA interference promotes cell survival in a human embryonic stem cell-derived HD model.[120] Furthermore, cultured rat striatal neurons exhibit a decrease in Rhes gene expression in presence of mHtt, and this decrease was interpreted as a compensatory response to an hypothetical factor promoting cytotoxicity.[117]

It has been proposed that Rhes effect on mHtt toxicity can stem from its influence on mHtt aggregation state. In presence of Rhes, mHtt forms less aggregates in cultured HEK293 cells and the soluble protein fraction increases.[116]

Rhes-induced mHtt preference for soluble state depends on its SUMOylation. SUMOylation of mHtt decreases the formation of aggregates and increases the amount of soluble, dispersed mHtt.[43] Rhes behaves as a SUMO E3 ligase and greatly increases SUMOylation of mHtt, while decreasing ubiquitination, when the proteins are over-expressed in HEK293 cells. It has been demonstrated that a causal relationship between Rhes-induced SUMOylation and cytotoxicity exists. In fact, Lys to Arg mutations at positions 6, 9, 15, and 91 of mHtt not only prevent SUMOylation by Rhes, but also prevent mHtt disaggregation and cell death. In addition, manipulations of SUMO1 in cultured cells expressing mHtt confirm that Rhes-mediated SUMOylation influences

mHtt cytotoxicity: depletion of SUMO1 by RNAi increased mHtt aggregates while decreasing the cytotoxicity due to Rhes, whereas over-expression of SUMO1 has opposite effects.[116] Since Rhes does not SUMOylate wild-type Htt, it is likely that the expanded polyQ stretch makes the protein more susceptible to SUMOylation. Steffan *et al.* showed that SUMOylation stabilizes mHtt and increases its concentration within the cell.[43] At the moment, the exact mechanism by which the dispersed SUMOylated mHtt is cytotoxic is unknown.

Golgi apparatus could have a role in mediating mHtt-Rhes toxicity as the Golgi protein ACBD3 (acyl-CoA binding domain containing 3) appears to function as a scaffold which binds physiologically mHtt and Rhes and promotes their interaction.[121] ACBD3 deletion abolishes HD neurotoxicity, that it conversely increased by ACBD3 overexpression.

Further evidence for a role of Rhes in HD neurodegeneration comes from the work of Okamoto *et al.* on synaptic *vs.* extrasynaptic NMDA receptors.[122] Whereas synaptic NMDA receptor activation can promote mHtt aggregation and increase cell viability, activation of extrasynaptic receptors has opposite consequences. Rhes protein expression may be modulated by these extrasynaptic receptors. In fact, when they are inhibited, Rhes expression decreases, suggesting that activation of extrasynaptic receptors, which causes neurodegeneration, increases Rhes expression. In the same study Okamoto *et al.* show that blocking of extrasynaptic NMDAR restores CREB and PGC-1 activity in a cellular model of HD and rescues the disease phenotype *in vivo* in a mouse YAC128 model of HD. At the moment, how changes in Rhes levels could affect CREB and PGC-1 activity, and how this correlates with symptomatic improvement *in vivo*, has still to be defined.

Finally, it has been discovered very recently that Rhes is able to activate autophagy independently of mTOR and that mHtt blocks Rhes-induced autophagy activation, presumably by sequestering Rhes and hampering it to fulfil its role in autophagy regulation.[123]

3. Aim of the study

Mitochondria are known to play a central role in Huntington's disease (HD) and several functional and morphological defects were documented for mitochondria in HD models. In addition, HD patients show metabolic alterations ascribable to mitochondrial loss of function. Despite the high number of related studies, it is still debated whether mitochondrial dysfunction represents just an epiphenomenon of the cellular degeneration or it has an actual pathogenic role.

The first aim of this study was to clarify whether mitochondrial impairment is a main trigger in HD neurodegeneration or a late event.

To address this issue a complete set of mitochondrial parameters, such as Ca^{2+} retention capacity, respiration, membrane potential and ROS concentration, was assessed. The study was carried out in striatal precursors expressing full length mutant Htt (mHtt) or transfected to express N-terminal mHtt. Bioenergetic parameters were also analyzed in brain mitochondria isolated from a mouse HD model at 12 month and 1 week of age.

As the data obtained from these analysis suggested that mutant mHtt only is not sufficient to induce mitochondrial damage, we wondered whether other non-mitochondrial factors could be involved. The striatal protein Rhes appeared as a likely candidate. This protein was recently proposed as an important mediator of mHtt cytotoxicity, even if the molecular mechanisms underlying Rhes-mHtt interplay have still to be understood.

Therefore, the second aim of this study was to investigate whether Rhes expression affects mitochondrial function in mHtt-expressing cells in order to discover whether it can be a contributor of mitochondrial damage in HD. With this goal, immortalized striatal precursors were transiently cotransfected to express both mHtt and Rhes. Afterwards the mitochondrial function of these cells was characterized in terms of mitochondrial membrane potential and ROS concentration. Concomitantly, studying its interaction with Rhes, the role of mHtt aggregation in the context of cell death was also investigated.

4. Materials and methods

4.1 Cell cultures and transfection

STHdhQ7 (Q7) and STHdhQ111 (Q111) clonal striatal cell lines were established from E14 striatal primordia of KI-Hdh Q111 and WT-Hdh Q7 littermate mouse embryos[124] and kindly provided by Ernesto Carafoli (Department of Biomedical Sciences, University of Padua). HEK293 (85120602, ECACC) are human embryonic kidney cells. Q7, Q111 and HEK293 cells were grown in Dulbecco's modified essential medium (D5761, Sigma) supplemented with 10% fetal bovine serum, 2 mM glutamine, 10 units/ml penicillin, 100 µg/ml streptomycin. Q7 and Q111 cells were maintained at the permissive temperature of 33 °C in a humidified incubator with 5% CO_2. HEK293 cells were maintained at 37°C in a humidified incubator with 5% CO_2.

Twenty-four hours after plating, the cells were transfected by lipofectamine (Lipofectamine 2000, Life Technologies) following manufacturer's instructions. Briefly, 1 µg of DNA and 2 µL of lipofectamine were added to 100 µL of optiMEM (Gibco) and distributed upon each well of a 24-well plate. After 2 hours of incubation, the transfection mix was replaced with fresh complete medium.

The cells were transfected with pRRLsin.PPTs.hCMV.GFPpre vector that codes for GFP protein or the same vector with human huntingtin exon 1 gene inserted upstream of GFP. Huntingtin exon 1 has 18Q or 150Q at the N-terminus. To perform the experiments on Rhes function, Q7 cells were cotransfected with pRRLsin.PPTs.hCMV.GFPpre vectors and empty pcDNA3.1 vector or pcDNA3.1 carrying the human Rhes gene. The total amount of DNA was maintained and equal quantities of the two plasmid DNA were used. Transfected cells were analyzed 48 hours after transfection.

4.2 Amplification and purification of plasmid DNA

4.2.1 Preparation of competent E. coli cells

DH10B E. coli cells were inoculated in a 10 mL overnight culture of Luria Bertani (LB) broth at 37°C. On the following morning, 1 L of LB broth was seeded with the 10 mL overnight culture. The culture was incubated at 37°C while shaking at 250 rpm until the optical density measured at 600 nm (OD_{600}) reaches 0.3-0.4. From this point forward, the remainder of the preparation was done in the cold room. The 1 L culture was split into 50 mL sterile tubes and the cells were pelleted by chilled centrifugation at 2500 g for 15 min. The supernatant LB broth was discarded and the pellet resuspended by gentle swirling with 100 mL of $CaCl_2$ 100 mM. The resuspended cells were incubated on ice for 30 min and then pelleted by chilled centrifugation at 2500 g for 15 min. The resuspension and centrifugation steps were repeated another time. Finally, the cell pellet was gently resuspended in 5 mL of $CaCl_2$ 100 mM plus 20% glycerol and divided into 60 µL aliquots. The aliquots were flash freezed in liquid nitrogen and stored at −80°C.

4.2.2 Transformation of E. coli

100 ng of plasmid DNA were added to one aliquot of competent DH10B E. coli cells. Another aliquot of competent cells was used as negative control. The DNA-cell mixture was incubated on ice for 30 min and then heat shocked by keeping it at 42°C in a termoblock for 90 sec. The aliquots were immediately returned to ice for 2 min. The cells were recovered by adding 900 µL of LB broth and incubating at 37°C while shaking at 250 rpm for 1 h. The cells were pelleted by centrifugation at 4000 g for 5 min. The two pellets was resuspended in a small volume of LB broth and distributed into previously prepared LB agar plates containing ampicillin 100 µg/ml. The plates were incubated in a stationary 37°C incubator to grow the bacterial colonies.

4.2.3 Amplification and purification of plasmid DNA from E. coli

One colony from LB agar plate seeded with transformed DH10B E. coli was collected and inoculated in a 250 mL overnight culture of LB broth at 37°C. On the following morning, the bacteria culture was centrifugated at 4000 rpm for 10 min and plasmid

DNA was extracted and purificated following the manufacturer's instructions of a commercial kit (PureLink HiPure Plasmid Maxiprep Kit, Life Technologies).

4.3 Oxygen consumption rate measurement

Q7 and Q111 cells (5000/well) were seeded onto Seahorse 24-well microplates 24 hours prior to the analysis on the Seahorse XF24 extracellular flux analyzer (Biosciences) following the manufacturer's instructions. All experiments were performed at 33°C. Oxygen consumption rate data consist of mean rates during each measurement cycles consisting of a mixing time of 30 sec and a waiting time of 3 min followed by a data acquisition period of 3 min. Rates displayed are basal respiration and rates following addition of 1 µg/ml oligomycin, 0.6 µM FCCP, 1 µM rotenone and 1 µM antimycin A. The FCCP concentration was previously determined as that optimal concentration to maximize the stimulation of mitochondrial respiration of Q cells.
The measured oxygen consumption rate was subsequently normalized to the number of viable plated cells using the calcein AM assay. Cell permeant non-fluorescent calcein AM dye is converted to the fluorescent calcein dye by intracellular esterase activity in live cells. The medium above Q cells was replaced with warm DMEM containing 3 µM calcein AM (Life Technologies). The plate was incubated at 33°C for 20 min. Images of each well were collected by an epifluorescence inverted microscope (Olympus IMT-2) and the number of fluorescent cells attached in the region probed by the extracellular flux analyzer was count.

4.4 Calcium Retention Capacity measurement

4.4.1 Isolation of mitochondria from cells

One 500 cm^2 plate of Q7 or Q111 cells was seeded 48 hours before the experiment. The culture medium was removed and the cells were washed once with chilled PBS. PBS was removed and the cells were detached using a scraper. The cell suspension was centrifugated at 600 g at 4°C for 10 min and then the pellet was resuspended in 1 mL of Isolation Buffer (IB: 250 mM sucrose, 10 mM Tris, 0.1 mM EGTA pH 7.4). The cell

suspension was homogenized by stroking it 35 times with a Teflon pestle in a 2 mL glass potter. During this procedure, the glass potter was kept on ice. The homogenate was centrifugated at 600 g for 10 min at 4°C and the collected supernatant was centrifugated at 7 000 g for 10 min at 4°C. The obtained pellet was resuspended in 500 µL of ice-cold IB and centrifugated at 7 000 g for 10 min at 4°C. The pellet containing mitochondria was resuspended in 50 µL of IB and its protein concentration was measured with Bradford method.

4.4.2 Isolation of mitochondria from forebrain

Mitochondria were isolated from the forebrain (brain minus cerebellum) of 1 week or 12 month-old YAC128 mice or their wild-type littermates. The cerebellum was excluded as it is usually not involved in HD pathology. The mouse was killed by cervical dislocation (adults) or decapitation (pups). The forebrain were rapidly excised and immediately placed in 10 mL of ice-cold Isolation Buffer (IB: 250 mM sucrose, 10 mM Tris, 0.1 mM EGTA pH 7.4) in a beaker, then it was washed 4 times with IB. The forebrain was minced into small pieces with scissors while keeping the beaker in an ice bath. The IB used during the mincing was discarded and replaced with 1 ml of ice-cold fresh IB. The suspension was homogenized by stroking it 35 times with a Teflon pestle in a 2 mL glass potter. During this procedure, the glass potter was kept on ice. The homogenate was centrifugated at 1500 g for 10 min at 4°C and the collected supernatant was centrifugated at 10 000 g for 10 min at 4°C. The obtained pellet was resuspended in 100 µL of IB and carefully transferred on the top of a Percoll gradient made of 400 µL of Percoll 40% in IB and 600 µL of Percoll 25% in IB. The Percoll gradient was centrifugated at 20 000 g for 30 min at 4°C. The pellet split up into two bands with the mitochondria concentrated in the bottom one. The collected mitochondria were resuspended in 1 mL of ice-cold IB and centrifugated at 10 000 g for 10 min at 4°C. The pellet was resuspended in 50 µL of IB and its protein concentration was measured with Bradford method.

4.4.3 Cell permeabilization

Two 75 cm^2 flasks of Q7 or Q111 cells were seeded 48 hours before the experiment. The culture medium was removed and the cells were washed once with chilled PBS.

PBS was removed and the cells were detached using a scraper. The cell suspension was centrifugated at 600 g for 10 min at 4°C and then the pellet was resuspended in 1 mL of the following buffer: 130 mM KCl, 5 mM mM phosphate buffer, 10 mM MOPS, 1 mM EGTA, pH 7.4. The protein concentration was measured with Bradford method. Digitonin 1 µM was added to the cell suspension that was then incubated at 4°C for 10 min. Afterwards it was centrifugated at 600 g for 10 min at 4°C and resuspended in CRC buffer (see next paragraph) supplemented with 10 µM cytochrome c to reach the concentration of 0.5 µg/µL.

4.4.4 Calcium Retention Capacity

Mitochondrial calcium retention capacity was measured fluorimetrically using Calcium Green-5N (Molecular Probes, excitation at 506 nm, emission at 535 nm) which increases its fluorescence emission upon binding extramitochondrial Ca^{2+}. Isolated mitochondria were diluted in CRC buffer (130 mM KCl, 5 mM phosphate buffer, 10 mM MOPS, 1 µM EGTA, 5 mM glutamate, 2.5 mM malate, 2.5 µM Calcium Green-5N, pH 7.4) to reach the concentration of 0.5 µg/µL. The suspension of isolated mitochondria or permeabilized cells was transferred in a 96-well dark plate, 100 µL in each well. Fluorescent emission of Calcium Green-5N was measured by Fluoroskan Ascent (Thermo Scientific) while 10 µM $CaCl_2$ pulses were automatically added every minute. When the permeability transition pore opened, a large increase in fluorescence was recorded due to release of accumulated Ca^{2+} from mitochondria. The mitochondrial calcium retention capacity was indicated as the added Ca^{2+} concentration that causes the permeability transition pore opening.

4.5 Fluorescence Microscopy

4.5.1 Measurement of mitochondrial membrane potential

Mitochondrial membrane potential ($\Delta\psi_m$) was measured using the cationic tetramethylrhodamine methyl ester probe (TMRM, Molecular Probes, λ_{exc} = 548 nm, λ_{em} = 574 nm). TMRM passes through the plasmatic membrane and accumulates selectively in the mitochondria due to the potential difference at the level of inner

mitochondrial membrane, so a highly selective, potential-dependent staining of mitochondria is obtained.

The cells were seeded on 24 mm coverslips and the day after they were transfected or cotransfected as indicated in the Results section (chapter 5). After 48 hours, the cells were incubated for 30 min at 37°C (or 33°C for Q cells) with 10 nM TMRM in DMEM supplemented with 2 mM glutamine and 16 μM cyclosporine H in order to block the multidrug-resistance pumps and avoid TMRM rejection by cells. Coverslip images were collected with an inverted microscope (Olympus IMT-2) equipped with a xenon lamp as a fluorescence light (75W), a 16 bit digital cooled CCD camera provided with a cooling system (Miromax, Princeton Instruments), a 40 x oil objective and appropriate excitation and emission filters. Several fields were acquired of each coverslip before and after addition of trifluorocarbonylcyanide phenylhydrazone (FCCP) 4 μM. FCCP provokes the $\Delta\psi_m$ collapse and the consequent TMRM discharge from mitochondria.

Images were analyzed using Image J software. Fluorescence intensity was measured in the regions of interest, defined as cell regions rich in mitochondria. For each analyzed coverslip TMRM fluorescence intensity was calculated as the difference between the mean fluorescence intensity before and after FCCP addition.

To measure the mitochondria susceptibility to oligomycin-induced depolarization, one image of a selected field of TMRM loaded cells was acquired every 4 min. Once the fluorescence intensity of the field was stable over time, 3 μM oligomycin was added and the fluorescence was followed for 32 min, afterwards 4 μM FCCP was added. Finally, the fluorescence intensity of each analyzed cell was plotted against time.

4.5.2 Measurement of oxidative stress

ROS concentration was measured using the cationic dihydroethidium probe (DHE, Sigma, λ_{exc} = 518 nm, λ_{em} = 605 nm). DHE freely permeates cell membrane and when it is oxidized, mainly by superoxide anion, it becomes red fluorescent. Oxidized DHE bind to nuclear DNA, a process that results in a further increase in fluorescence. DHE produces diffuse labeling throughout the cells including nucleolar and nuclear regions, mitochondria, lysosomes, and the cytosol.

The cells were seeded on 24 mm coverslips and the day after they were transfected or cotransfected as indicated in the Results section (chapter 5). After 48 hours, the cells were incubated for 20 min at 37°C (or 33°C for Q cells) with 5 μM DHE in HBSS.

Then the DHE solution was replaced with HBSS. When indicated, cells were incubated for 15 min at 37°C (or 33°C for Q cells) with 100 μM H_2O_2 in HBSS before DHE loading. Coverslip images were collected with an inverted microscope (Olympus IMT-2) equipped with a xenon lamp as a fluorescence light (75W), a 16 bit digital cooled CCD camera provided with a cooling system (Miromax, Princeton Instruments), a 40 x oil objective and appropriate excitation and emission filters. Several fields were acquired of each coverslip. Images were analyzed using Image J software. Fluorescence intensity was measured in the regions of interest (ROIs) corresponding to the whole cell. For each analyzed coverslip DHE fluorescence intensity was calculated as the mean fluorescence of all the selected ROIs.

4.5.3 Immunofluorescence

Rhes protein in cotransfected Q7 cells were stained with anti-Rhes antibody. Q7 cells were seeded on 15 mm coverslips and the day after they were cotransfected with –GFP constructs and Rhes. After 48 hours, the cells were fixed with paraformaldehyde 4% for 20 min and permeabilized with Triton 0.2% in PBS for 10 min. Then they were saturated with BSA 4% in PBS for 1 h. All these steps were performed at room temperature. Saturated cells were incubated with mouse anti-Rhes antibody (GeneTex) 1:100 in BSA 0.5% overnight at 4°C. The cells were washed 3 times with PBS for 10 min and then incubated with Alexa Fluor 647 goat anti-mouse IgG antibody (Life Technologies) 1:100 in BSA 0.5% for 30 min at room temperature. The washing steps were repeated. The cells were finally incubated with 10 μM Hoechst 33342 (Sigma) 10 min at room temperature and the coverslips were mounted onto glass slides using ProLong Gold Antifade Reagent (Life Technologies). Images were collected using a confocal microscope (Leica SP5), a 63 x oil objective and appropriate emission filters.

4.6 Determination of cell death

4.6.1 Assessment of necrosis

The cells were seeded in a 24-well plate and the day after they were transfected or cotransfected with the constructs indicated in each experiment in the Results section

(chapter 5). After 48 hours, the cells were detached using trypsin 1 % and centrifugated at 600 g for 4 min at room temperature. The pellet obtained from a single well was resuspended in 500 μL of propidium iodide 10 μM in HBSS and incubated for 5 min at room temperature. The cell suspension was analyzed by flow cytometry (FACS Canto II, BD Biosciences): the instrument collected 5000 cells from the sample and measured their fluorescence emission in the red and green spectral regions. The green emission is given by GFP protein expressed by the transfected cells, while propidium iodide enters and marks as red-fluorescent only the cells whose plasma membrane is not intact. Thus, the percentage of dead cells was calculated from the ratio between the number of propidium iodide-positive transfected cells and the total number of transfected cells.

4.6.2 Assessment of apoptosis

The extent of apoptosis induced by Rhes in cotransfected Q7 cells was measured using Hoechst 33342, a cell-permeant nuclear dye that emits blue fluorescence when bound to DNA. It can be used to detect cell apoptosis as the chromatin condensation that associates with this process determines an increase in fluorescence of the nucleus.
Q7 cells were seeded in a 24-well plate and the day after they were cotransfected with –GFP constructs and Rhes or the corresponding empty vector. After 48 hours, the cell were incubated 10 min with 10 μM Hoechst 33342 (Sigma) in DMEM at 37°C. The Hoechst medium was then replaced with DMEM and the cells were immediately analyzed by an inverted microscope (Olympus IMT-2) equipped with a 20 x air objective and appropriate excitation and emission filters. Several fields were acquired of each well. Images were analyzed using Image J software. The percentage of apoptotic cells was calculated from the ratio between the number of transfected cells (those that emitted green fluorescence) that showed highly fluorescent nuclei and the total number of transfected cells.

4.7 Filter retardation assay

The amount of SDS-insoluble aggregates formed by mHtt exon 1 in presence or absence of Rhes was quantified by filter retardation assay. Q7 cells were seeded in a 6-well plate and the day after they were cotransfected with 150Q-Httexon1-GFP and Rhes or the

corresponding empty vector. After 48 hours, the cells were detached using trypsin 1 % and centrifugated at 600 g for 4 min at room temperature. The pellet obtained from a single well was resuspended in 100 µL of the following Lysis Buffer: NP-40 1%, sodium deoxycholate 0.25%, EDTA 2 mM, β-mercaptoethanol 0.5%, SDS 2% in PBS. Samples were homogenized by three passages through a 0.5 mm needle, diluted in Lysis Buffer as indicated in figure 15A and heated at 100°C for 5 min. Afterwards, 6 µL of each sample were applied with 45 sec of vacuum suction onto a 0.2 µm nitrocellulose membrane (BioRad) previously soaked with SDS 2% in PBS. The membrane was immunoblotted with anti-GFP antibody (Santa Cruz Biotechnologies) as described in the next paragraph.

The transfection efficiency, as measured by flow cytometry, did not vary significantly when Q7 are cotransfected with 150Q-Httexon1-GFP and Rhes or the corresponding empty vector. Thus, it can be excluded that the detected difference in aggregate formation is due to different transfection efficiencies.

4.8 Cell extracts and western blot analysis

4.8.1 Sample preparation

To obtain the western blot of figure 9B, 13A and 15C, the cells were seeded in a 6-well plate and the day after they were transfected or cotransfected with the constructs indicated in each experiment in the Results section (chapter 5). After 48 hours, the cells were detached using trypsin 1 % and centrifugated at 600 g for 4 min at room temperature. The pellet obtained from a single well was resuspended in 100 µL of the following Lysis Buffer: NP-40 1%, sodium deoxycholate 0.25%, EDTA 2 mM, β-mercaptoethanol 0.5%, SDS 2%, 1 x protease inhibitor mix (Roche) in PBS. Samples were homogenized by three passages through a 0.5 mm needle and their protein concentration was determined with Bradford method. Then 25 µL of Sample Buffer 4 x (glycerol 20%, SDS 3%, Tris 75 mM, bromophenol blue 0.02%, β-mercaptoethanol 5% in H_2O, pH 6.8) were added and the samples were heated at 100°C for 5 min. Finally they were loaded on the gel or stored at -20°C.

To obtain the western blot of figure 16B, the cell pellet of cotransfected Q7 cells was resuspended in 100 µL of PBS supplemented with EDTA 2 mM and 1 x protease

inhibitor mix (Roche). The cells were lysated by 3 cycles of freezing in liquid nitrogen and thawing at room temperature. Samples were centrifugated at 12 000 g for 10 min at 4°C and the two obtained fractions, pellet and supernatant, were processed separately. The protein concentration of the supernatant was determined with Bradford method, then 25 µL of Sample Buffer 4 x were added and the samples were heated at 100°C for 5 min. The pellet was resuspended in 30 µL of the above Lysis Buffer plus 1x Sample Buffer, it was homogenized by three passages through a 0.5 mm needle and then heated at 100°C for 5 min. The pellet and the supernatant fraction were loaded in two separate gels or stored at -20°C.

4.8.2 SDS-polyacrylamide gel electrophoresis (SDS-PAGE) and immunoblot

Electrophoresis was performed on polyacrylamide gel prepared in glass slabs 1 mm thick with 12% acrylamide in the separating gel and 4% in the stacking gel. The following solutions were used for the preparation of the gel and the electrophoresis run:

Acrylamide/bisacrylamide: 30% acrylamide and 0.8% bisacrylamide
Lower Tris-HCl (4x): 1.5 M Tris-HCl and 0.4% SDS, pH 8.8
Upper Tris-HCl (4x): 0.5 M Tris-HCl and 0.4% SDS, pH 6.8
Running buffer (4x): 0.1 M Tris-HCl, 0.77 M glycine and 0.4% SDS, pH 8.3

The polymerization of the gel was obtained by the addition of TEMED (Sigma) and ammonium persulfate 0.1 mg/ml (Sigma). Samples were run on the gel at room temperature using an Electrophoresis Power Supply (Apelex) that provided a constant voltage of 150 V in the stacking gel and 200 V in the separating gel.
In order to make the proteins accessible to antibody detection, they were moved from within the gel onto a nitrocellulose membrane. Once the samples finished the run, the gel was washed from the excess SDS with Transfer Buffer (Tris 25 mM, glycine 192 mM, methanol 20%, pH 8.0). A 0.45 µm nitrocellulose membrane (BioRad Laboratories) was placed on top of the gel, avoiding creating bubbles, and a stack of tissue papers placed on top. This stack was then inserted into a transfer box filled with Transfer Buffer, so that the gel is oriented towards the cathode and the membrane towards the anode. When a current is applied to the electrodes, this causes the proteins to migrate from the negatively charged cathode to the positively charged anode, i.e.

towards the membrane. The separating and the stacking part of the gel were transferred separately: the former was transferred 17 h with 150 mA of current, while the latter 24 h with 150 mA of current plus 4 h at 400 mA in order to let the high molecular weight aggregates pass on the nitrocellulose membrane. The transfer was performed at 4°C.
Once the transfer was carried out, the membrane was saturated with fat-free milk 5% in TBS (Tris-HCl 50 mM, NaCl 150 mM, pH 7.5) for 1 h at room temperature. The antibodies used to detect the proteins of interest were diluted in milk 1% in TBS. The following primary antibodies were used:

Rabbit Anti GFP (Santa Cruz Biotechnologies), dilution 1 : 1000
Mouse Anti-Rhes (GeneTex), dilution 1 : 500
Mouse Anti β-actin (Abcam), dilution 1 : 2000

All the primary antibody incubations were carried out overnight at 4°C. Following the incubation, membranes were washed 3 times for 10 min with Washing Buffer (Tris-HCl 50 mM, NaCl 85 mM, Tween 20 0.1%, pH 7.5). Secondary antibodies were diluted in milk 1% in TBS and incubated with the membrane for 1 h at room temperature. Secondary antibodies used were:

Rabbit Anti-Mouse (BioRad), dilution 1 : 2000
Mouse Anti-Rabbit (BioRad), dilution 1 : 2000

Finally membranes were washed 3 times for 10 min with Washing Buffer.

4.8.3 Chemiluminescent detection

Membranes were exposed to LiteAblot PLUS Enhanced Chemiluminescent Substrate (EuroClone) for 1 min. This incubation causes the generation of luminous signal due to the oxidation of the substrate by horseradish peroxidase bound to the secondary antibody. The light, emitted at λ_{max} 340 nm, was detected by a CCD camera (Image Station 440 CF, Kodak).

4.8.4 Densitometry

Images of the acquired western blots were analyzed using the Image J software. This program allows the quantification of the optical density of bands or dots that is directly proportional to the protein content.

4.9 Statistics

Results are presented as mean ± standard deviation. When the experiment was repeated more than 3 times, comparisons between two groups of data were performed via 2-tailed unpaired Student t test. A P-value less than 0.05 was taken to indicate a significant difference that was then tagged with an asterisk.

5. Results

5.1 Mitochondrial function in cells stably expressing full length mutant Htt

The effects of stable expression of full length mutant huntingtin (mHtt) on mitochondria functions were studied in a commonly used HD model, *i.e.* immortalized striatal neuron precursors established from a HD knock-in mouse model (Hdh^{Q111}) and wild-type mice (Hdh^{Q7})[125]. $STHdh^{Q111/\ Q111}$ cells (Q111 from now on) homozygously express full length mHtt having 111 glutamines at the N-terminus, while $STHdh^{Q7/\ Q7}$ cells (Q7) express the wild-type form with 7 glutamines.

5.1.1 Q111 mitochondria have a lower spare respiratory capacity

In situ mitochondrial respiration of plate-attached Q7 and Q111 cells was monitored by using an extracellular flux analyzer. Five parameters of respiration were measured: (1) basal respiration, (2) respiration driving mitochondrial H^+ leak (after oligomycin addition), (3) maximal respiration (after FCCP addition), (4) respiration supported by electron flow through complex II (after rotenone addition), (5) non-mitochondrial respiration (after antimycin A addition) (Fig. 6).

Q111 cells showed the same basal respiration as Q7 cells, and we did not detect any significant difference also in the respiration parameters (2), (4) and (5). However, when FCCP stimulated the maximal respiration by uncoupling the electron transport chain from ATP synthesis, Q111 mitochondria proved to be significantly less able to upregulate the electron transport chain activity. Specifically, the spare respiratory capacity, given by the difference between maximal and basal respiration, is 28% lower in Q111 cells than in Q7 cells.

Thus, mHtt impairs electron transport chain activity in Q111 cells and this defect arises when mitochondria are required to do an extra effort, such as that of ATP generation. This deficiency could turn out to be particularly harmful to neurons as they change continuously the rate of ATP synthesis to match their energy-expensive physiological functions.

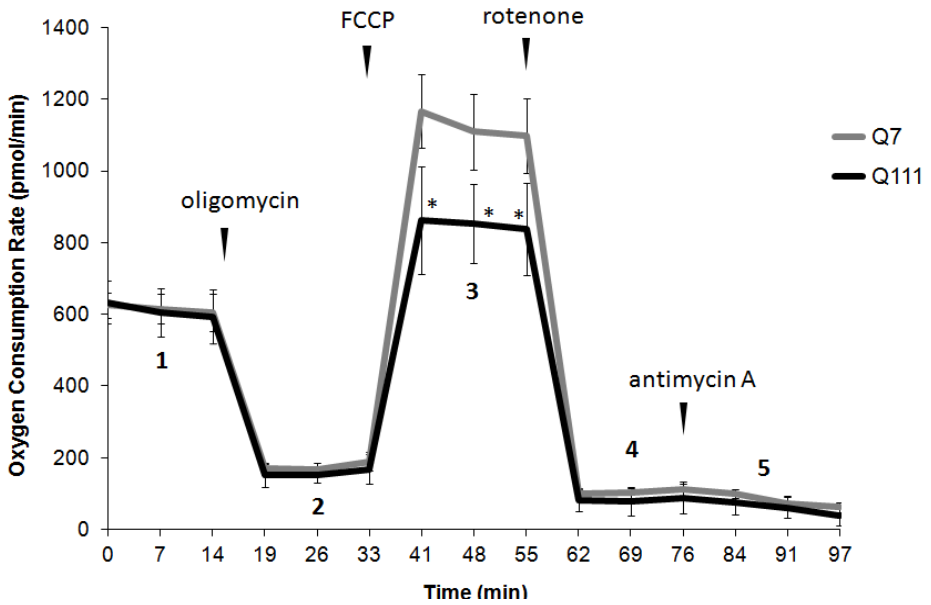

Fig. 6. Oxygen consumption rate of Q7 and Q111 cells measured by extracellular flux analyzer. Cells were stressed with different stimuli to reveal possible respiratory defects: oligomycin to block ATP synthase, FCCP to uncouple the electron transport chain from ATP synthesis, rotenone and antimycin A to inhibit complex I and III, respectively. The measured oxygen consumption rate was subsequently normalized to the number of viable plated cells using the calcein AM assay.

5.1.2 Q111 mitochondria are more susceptible to oligomycin-induced depolarization

As reported by Lim *et al.* Q7 and Q111 cells show only a minor difference in mitochondrial membrane potential ($\Delta\psi_m$)[126]. However, a defective electron transport chain may not lead to a detectable decrease in $\Delta\psi_m$ if this defect is compensated by ATP synthase reversal. ATP synthase can invert its normal activity and hydrolyze ATP while pumping proton out of the matrix in order to sustain the proton gradient. Thus, to check whether in Q111 cells a lower activity of the electron transport chain is masked by the compensation of ATP synthase, $\Delta\psi_m$ was measured with TMRM fluorescent probe after treatment with oligomycin, an ATP synthase inhibitor (Fig. 7). Among all the analyzed cells (40 for each cell type in 3 different experiments), 36% of Q111 showed a drop of $\Delta\psi_m$ after blocking ATP synthase *versus* 2,6 % of Q7 cells. Therefore, in Q111 cells mHtt expression results in a lower activity of the electron transport chain and this defect is partially compensated by ATP synthase reversal.

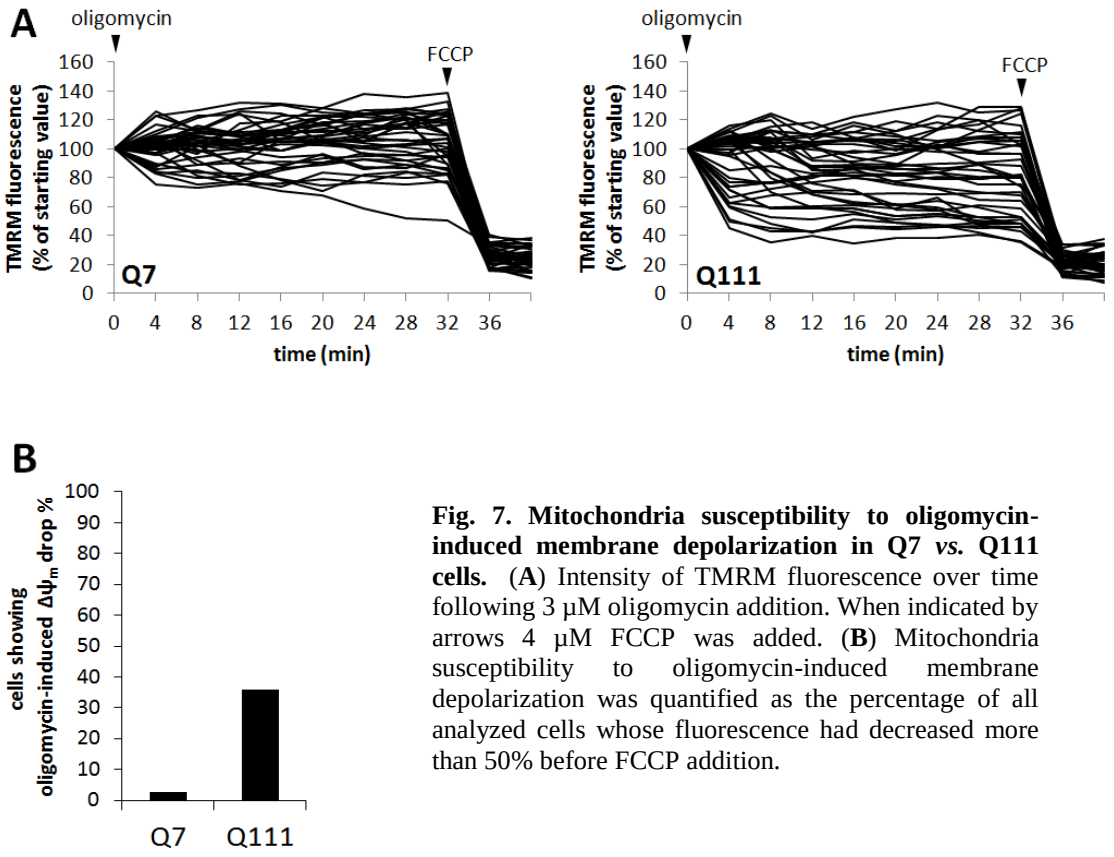

Fig. 7. Mitochondria susceptibility to oligomycin-induced membrane depolarization in Q7 *vs.* Q111 cells. (**A**) Intensity of TMRM fluorescence over time following 3 µM oligomycin addition. When indicated by arrows 4 µM FCCP was added. (**B**) Mitochondria susceptibility to oligomycin-induced membrane depolarization was quantified as the percentage of all analyzed cells whose fluorescence had decreased more than 50% before FCCP addition.

5.1.3 Q111 and YAC182 brain mitochondria have a higher calcium retention capacity

To evaluate whether the defective electron transport chain impinges on mitochondrial Ca^{2+} uptake in Q111 cells, we measured the calcium retention capacity (CRC) of mitochondria isolated from Q111 cells and their wild-type counterparts (Fig. 8A). CRC was quantified as the external [Ca^{2+}] at which matrix [Ca^{2+}] triggers the permeability transition pore (PTP) opening. This is reflected by an abrupt release of accumulated Ca^{2+} that is monitored by using Calcium Green-5N, an indicator that does not enter mitochondria and exhibits an increase in fluorescence emission upon binding Ca^{2+}. The external [Ca^{2+}] was gradually increased and mitochondria take up this Ca^{2+} until a sudden increase in fluorescence indicated PTP opening.

The CRC measurement was performed also using digitonin-permeabilized Q7 and Q111 cells (Fig. 8A), an additional model where the cellular context is partially preserved. Digitonin treatment permeabilizes both mitochondrial and endoplasmic reticulum membranes, so any contribution of the endoplasmic reticulum can be excluded.

Surprisingly, in both models, Q111 mitochondria proved to be much more resistant to Ca^{2+}-induced opening of PTP.

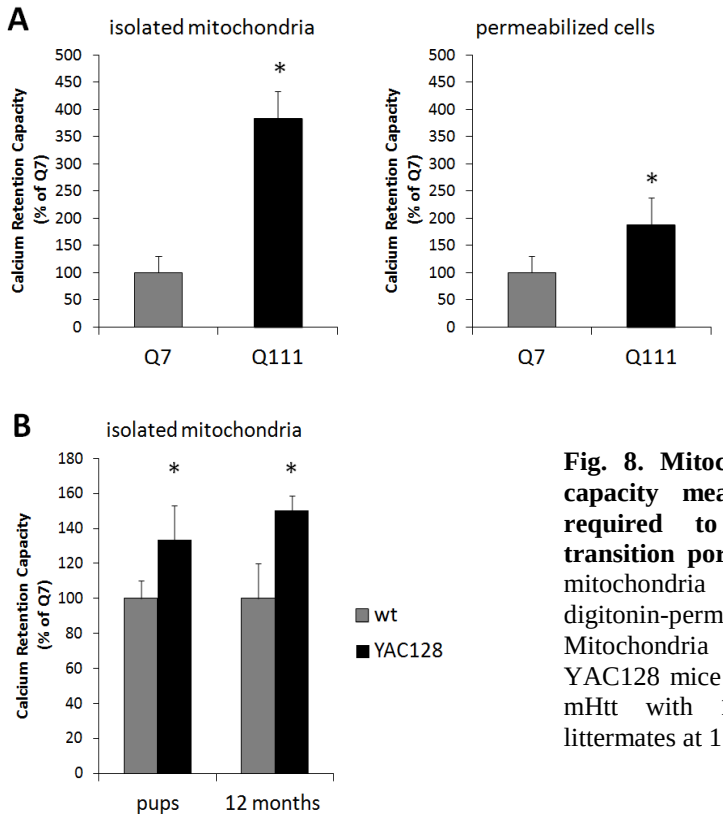

Fig. 8. Mitochondrial calcium retention capacity measured as external [Ca^{2+}] required to open the permeability transition pore. (**A**) Q7 *vs*. Q111 isolated mitochondria (*left*) and Q7 *vs*. Q111 digitonin-permeabilized cells (*right*). (**B**) Mitochondria isolated from forebrain of YAC128 mice expressing full-length human mHtt with 128Q and their wild-type littermates at 1 week or 12 months of age.

This evidence was strengthened by CRC measurements on isolated mitochondria from the forebrain of YAC128 mice and their wild-type littermates (Fig. 8B). YAC128 is a yeast artificial chromosome mouse model of HD with the entire human HD gene containing 128 CAG repeats. It is reported that, starting from 6th month of age, YAC128 mice develop motor abnormalities and brain atrophy including cortical and striatal atrophy associated with striatal neuronal loss.[127]

Isolated mitochondria from YAC128 mice showed a higher CRC when compared with mitochondria from wild-type mice, in agreement with the results obtained in Q111 and Q7 cells. This applies to 12-month-old mice but, remarkably, even to 1-week-old pups when the disease phenotype is far from being developed. Thus, it seems that very soon in disease progression mitochondria develop a higher resistance to permeability transition.

To date, studies of mitochondrial Ca^{2+}-loading capacity in HD have provided conflicting results, with some reports claiming that mHtt decreases the mitochondrial CRC.[71, 72] As highlighted elsewhere,[128] measurements of Ca^{2+} handling on isolated

mitochondria can be seriously affected by differences in methodological approaches. Mitochondria concentration, proportion of synaptic *vs.* non- synaptic or neuronal *vs.* glial mitochondria, as well as presence of PTP effectors in the resuspension buffer can condition the experimental outcomes. Differences in these parameters may account for some of the discrepancies present in the published literature concerning the Ca^{2+}-loading capacity of HD mitochondria.

To exclude that our data could be influenced by the buffer composition, we repeated CRC measurements on isolated mitochondria from Q cells and YAC128 mice with two different incubation buffers previously used in works that show opposite results:[71, 72, 91] 1) a buffer with succinate instead of glutamate and malate as energy source. Since complex II was observed to be less expressed in HD,[129] fuelling mitochondria with its direct substrate could potentially reveal this defect; 2) a buffer including Mg^{2+} and ATP, two PTP inhibitors. With both these buffers, the obtained results were comparable with those reported in Fig. 8.

Therefore, both cell and animal HD models showed that mHtt enhances the mitochondria resistance to PTP opening. Brustovetsky *et al.* obtained analogue results with mitochondria isolated from knock-in HD mouse models carrying 92 or 111 glutamines in the polyQ expansion.[90] The authors proposed that the cause of this unexpected result has to be ascribed to a compensatory response of mitochondria that adapt to the stressful environment produced by mHtt accumulation by protecting themselves and their host cells from the deleterious consequences of permeability transition.

5.2 Mitochondrial function in cells transiently expressing N-terminal mutant Htt

The information collected about mitochondrial function in Q7 and Q111 cells suggested that this chronic HD model, even if close to patient cells in reproducing the chronic feature of mHtt expression, may not be the best choice to dissect mHtt effects on mitochondrial function as it makes hard to distinguish between direct effects of mHtt expression and adaptive changes.

To rule out adaptive changes, mitochondrial alterations in HD were then studied in Q7 and HEK293 cells transiently transfected with non-inducible constructs bearing Htt exon 1 with 18 (wild-type form) or 150 (mutant form) glutamines at the N-terminus. Htt

exon 1 gene is fused with GFP gene at the C-terminus, thus a construct that codes for GFP served as a control in all the experiments.

The transient nature of mHtt expression allowed to focus on its short term consequences and the expression of N-terminal only, instead of the full length protein, limited our study to the damage mechanisms that involve the first N-terminal portion of mHtt. Mutant Htt is known to be cleaved by several proteases producing a wide range of short N-terminal fragments (cf. paragraph 2.1.2). These are thought to be the key player in HD pathogenesis, in fact, they are more prone to aggregation and more toxic than the full length protein. In addition, when mHtt N-terminal fragments are expressed in cell or animal models, they reproduce the most severe traits of full length mHtt toxicity.[130]

In all the experiments transfected Q7 and HEK293 cells were analyzed 48 hours after transfection when the maximum level of overexpression is reached.

5.2.1 N-terminal mutant Htt forms aggregates and is cytotoxic

As expected,[131] N-terminal mHtt forms large, easily visible and SDS-insoluble inclusions within HEK293 and Q7 transfected cells (Fig. 9). Confocal images indicated that mHtt aggregates are cytosolic and occasionally show a perinuclear distribution (*data not shown*).

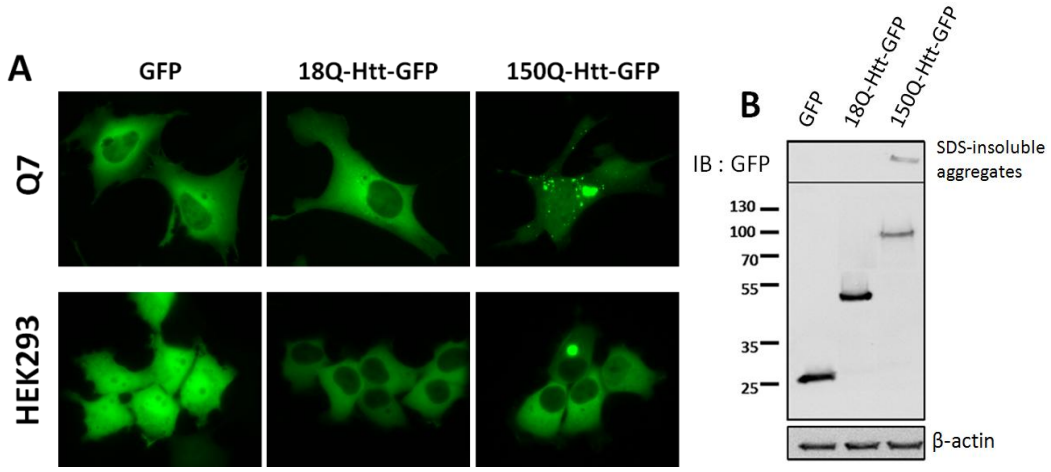

Fig. 9. N-terminal 150Q-Htt forms aggregates. (**A**) Fluorescence images of Q7 and HEK293 transfected cells: cytosolic aggregates of N-terminal 150Q-Htt are visible in both the cell lines. (**B**) Lysates of Q7 transfected cells immunoblotted with anti-GFP antibody: N-terminal 150Q-Htt forms SDS-insoluble aggregates that fail to enter the polyacrylamide gel.

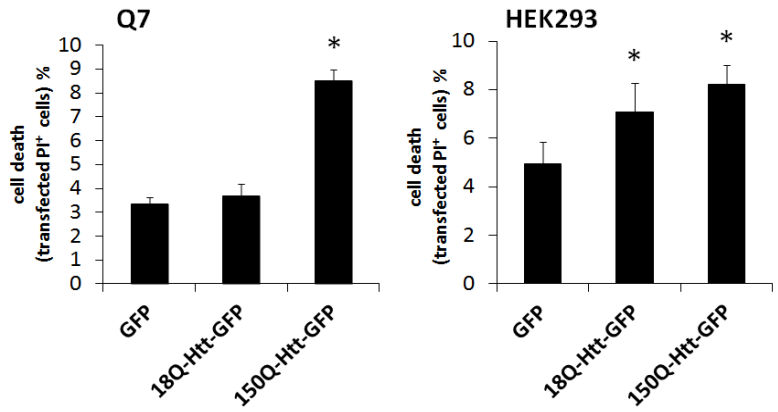

Fig. 10. Cell death of transfected Q7 and HEK293 cells. The percentage of dead cells was quantified by flow cytometry from the ratio between propidium iodide-positive transfected cells and the total number of transfected cells.

Cell death analysis of transfected cells showed that N-terminal mHtt significantly decreases cell survival in both the cell lines (Fig. 10). In HEK293 cells N-terminal wild-type Htt seems to be toxic too. Seredenina *et al.* similarly reported that wild-type Htt overexpression in infected primary neurons is cytotoxic and this effect disappears with milder infection conditions.[117] It is likely that wild-type Htt might mimic the mutant form when it is highly expressed. Consistently, we observed that N-terminal wild-type Htt can form aggregates, just as the mutant form, if it is expressed at high level by the transfected cell.

5.2.2 N-terminal mutant Htt affects neither mitochondrial membrane potential nor ROS concentration

Mitochondrial function in transfected Q7 and HEK293 cells were characterized by measuring mitochondrial membrane potential and ROS concentration (Fig. 11 and 12). No significant alteration was detected, irrespectively of which form of Htt was expressed. Therefore, even if N-terminal mHtt increases cell death, this does not seem to associate with mitochondrial impairment.

In the case of transfected Q7 cells, ROS concentration was assessed with both DHE and Mitotracker Red probe. The first probe has a widespread cellular distribution, while the second one specifically accumulates inside mitochondria. Even by using Mitotracker Red, mHtt does not induce an increase in oxidative stress (*data not shown*).

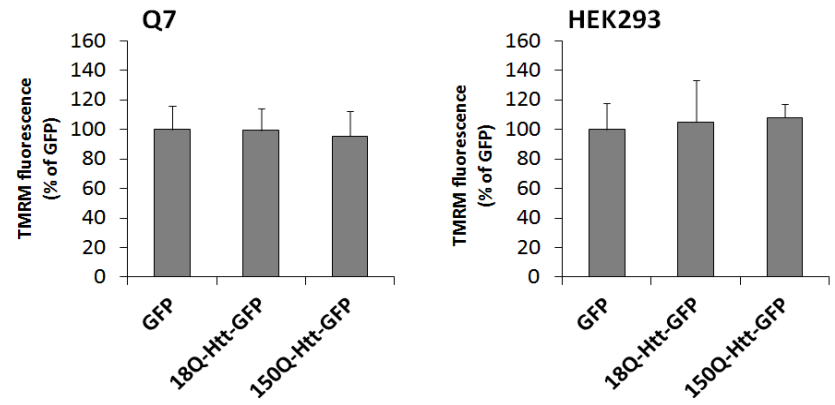

Fig. 11. Mitochondrial membrane potential of transfected Q7 and HEK293 cells measured by microscopy as fluorescent intensity of TMRM probe.

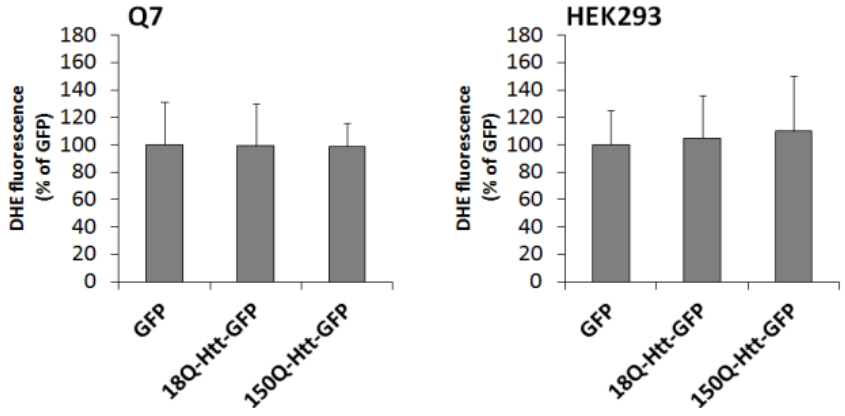

Fig. 12. ROS concentration of transfected Q7 and HEK293 cells measured by microscopy as fluorescent intensity of DHE probe.

In order to understand whether the lack of mHtt effect on mitochondria depend on its expression level, we repeated the above analysis at higher levels of expression in HEK293 cells (Fig. 13). A remarkable increase in exogenous protein expression was obtained by doubling the transfection mix of DNA and lipofectamine. In these conditions of 'high expression', N-terminal mHtt is considerably cytotoxic and it also causes loss of mitochondrial membrane potential and increase in ROS concentration.

Therefore, a threshold of expression can be described above which mHtt actually damages mitochondria. However this threshold is clearly much higher than the level of endogenous expression.

These data made us hypothesize that the endogenous levels of mHtt is not likely to affect mitochondrial function as a primary effect and that the occurrence of mitochondrial abnormalities might require additional non-mitochondrial stress factors.

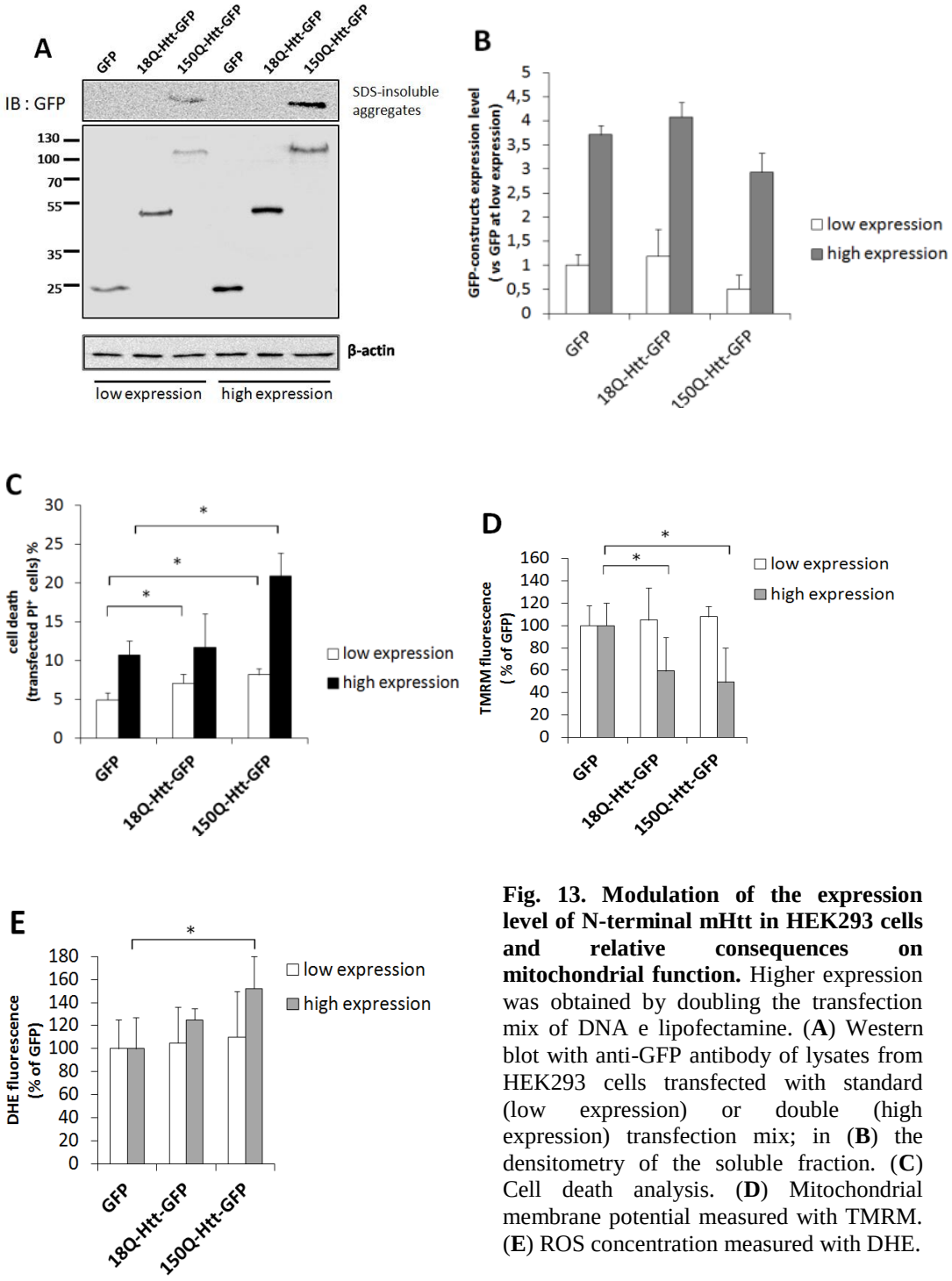

Fig. 13. Modulation of the expression level of N-terminal mHtt in HEK293 cells and relative consequences on mitochondrial function. Higher expression was obtained by doubling the transfection mix of DNA e lipofectamine. (**A**) Western blot with anti-GFP antibody of lysates from HEK293 cells transfected with standard (low expression) or double (high expression) transfection mix; in (**B**) the densitometry of the soluble fraction. (**C**) Cell death analysis. (**D**) Mitochondrial membrane potential measured with TMRM. (**E**) ROS concentration measured with DHE.

5.3 Mitochondrial function in cells transiently coexpressing N-terminal mutant Htt and Rhes

Since N-terminal mutant Htt seems not to cause *per se* those mitochondrial alterations that are largely documented in HD studies,[125] we wondered whether other factors could be involved. Rhes protein drew our attention, because it has been recently proposed as an important mediator of mHtt cytotoxicity[116] and it is not expressed in the cell models studied by us so far. It has been demonstrated that Rhes increases mHtt-induced cell death, but it is still unknown whether this effect implies a mitochondrial damage. In order to investigate whether Rhes expression affects mitochondrial function in mHtt-cells, we transiently cotransfected Q7 cells with GFP / 18Q-Httexon1-GFP / 150Q-Httexon1-GFP constructs and Rhes construct or the corresponding empty vector.

5.3.1 Rhes increases mHtt cytotoxicity and decreases mHtt aggregation

Firstly, we confirmed that Rhes increases mHtt cytotoxicity in Q7 cotransfected cells (Fig. 14A), as well as in Q111 cells that endogenously express the full length form of mHtt (Fig. 14B). Sbodio *et al.*[121] and Seredenina *et al.*[117] reported similar results by overexpressing an N-terminal fragment of mHtt containing 171 amino acids besides the polyQ tract. Here we show that Rhes is effective even with a much smaller mHtt fragment (78 amino acids).

Rhes significantly increases apoptosis when coexpressed with N-terminal mHtt (Fig. 14C), in agreement with the reported increase in cleaved caspase-3.[116] However, in this cell model Rhes induces apoptosis also in the presence of wild-type Htt. As previously discussed (cf. paragraph 5.2.1), this lack of specificity between mutant and wild-type form might be ascribed to the overexpression of the transfected vectors: in fact, also wild-type Htt can be harmful to the cell when it is expressed at high concentration.

According to Subramaniam *et al.*, Rhes facilitates mHtt neurotoxicity by SUMOylating it. SUMOylated mHtt forms less aggregates and this decrease in aggregation correlates with an augmented toxicity. [116]

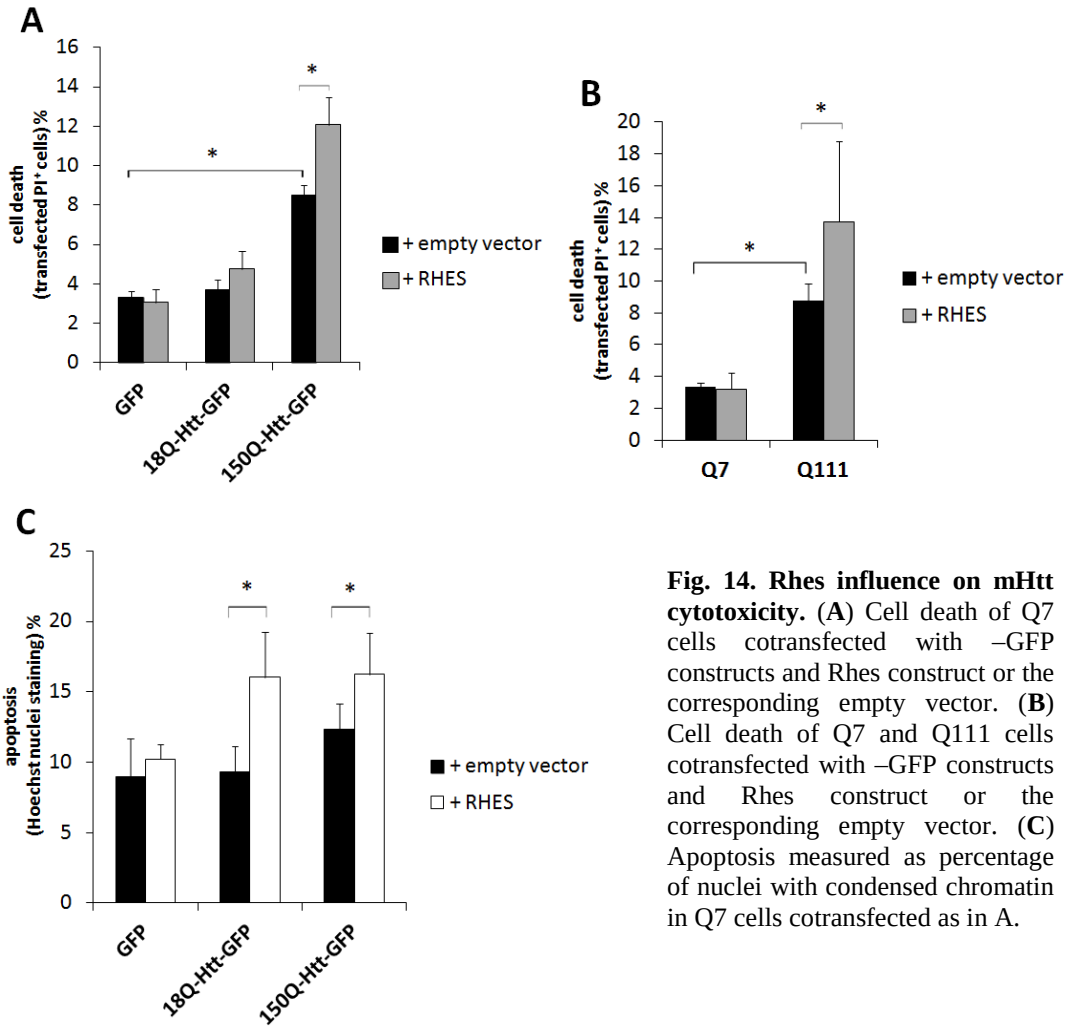

Fig. 14. Rhes influence on mHtt cytotoxicity. (**A**) Cell death of Q7 cells cotransfected with –GFP constructs and Rhes construct or the corresponding empty vector. (**B**) Cell death of Q7 and Q111 cells cotransfected with –GFP constructs and Rhes construct or the corresponding empty vector. (**C**) Apoptosis measured as percentage of nuclei with condensed chromatin in Q7 cells cotransfected as in A.

To check whether Rhes influences the mHtt aggregation state in this cell model, SDS-insoluble aggregates formed by N-terminal mHtt in absence or presence of Rhes were quantified by filter retardation assay as described in Material and Methods (Fig. 15A and B). Briefly, Q7 cells were cotransfected with 150Q-Htt-GFP construct and Rhes construct or the corresponding empty vector. After 48 hours from transfection, the cell lysates were filtered through a SDS-soaked nitrocellulose membrane to capture polyQ aggregates and the membrane was probed with anti-GFP antibody. Rhes expression provokes a 50% decrease in the aggregate amount while the soluble fraction of mHtt does not change in presence of Rhes, as quantified by western-blotting the above cell lysates with anti-GFP antibody (Fig. 15C and D). Surprisingly, Rhes lowers the concentration of the coexpressed GFP and 18Q-Htt-GFP proteins. An increased clearance by the ubiquitin-proteasome system could be a possible explanation of this reduction in protein levels. This hypothesis was excluded because, when the transfected cells were treated with a proteasome inhibitor (MG132), we still measured a remarkable

difference in the concentration of –GFP proteins in absence or presence of Rhes (*data not shown*), similarly to what shown in Fig. 15C and D.

Very recently it has been discovered that Rhes is able to activate autophagy[123] and this might actually account for the observed changes in protein level. Next experiments will be aimed at verifying this possibility.

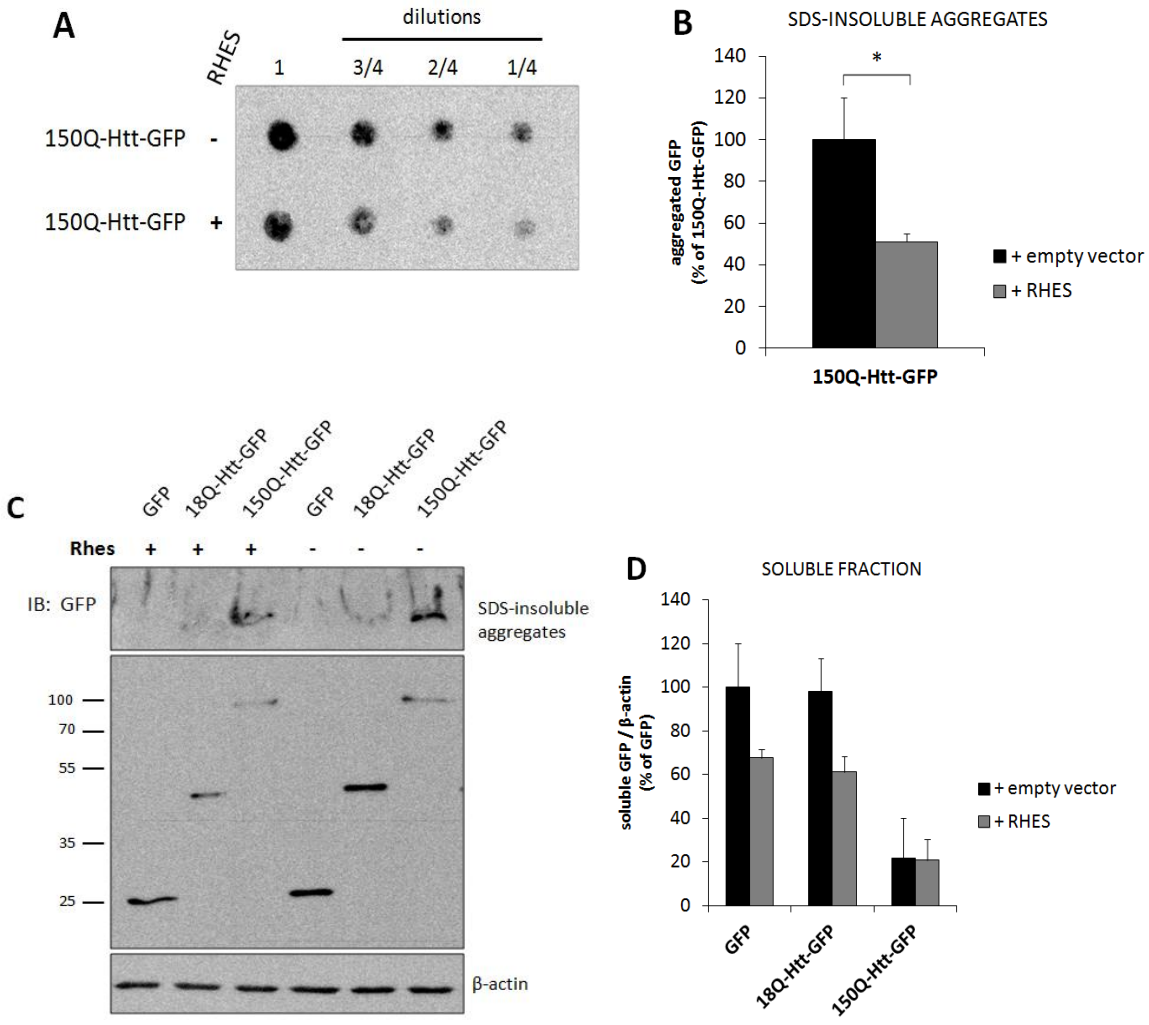

Fig. 15. Rhes effect on mHtt aggregation. (**A**) Filter retardation assay of N-terminal mHtt SDS-insoluble aggregates in presence or absence of Rhes. Lysates of Q7 cells cotransfected with 150Q-Htt-GFP construct and Rhes construct or the corresponding empty vector were filtered through a SDS-soaked nitrocellulose membrane to capture polyQ aggregates. The samples were dot-blotted at four different concentrations and probed with anti-GFP antibody. (**B**) Quantification of filter retardation assay A. (**C**) Western blot with anti-GFP antibody of lysates from Q7 cells cotransfected with –GFP constructs and Rhes construct or the corresponding empty vector, in (**D**) the densitometry of the soluble fraction.

5.3.2 Rhes colocalizes with and is sequestered by mHtt aggregates

Rhes protein overexpressed by Q7 cells is mostly cytosolic but it can also localize on the plasma membrane, as observed by Vargiu *at al.* in PC12 cells.[108] When coexpressed with N-terminal mHtt, Rhes can localize around its aggregates (Fig. 16A). It is interesting to point out that an analogous localization has been reported for SUMO-1, [43] that is the known substrate of mHtt SUMOylation catalyzed by Rhes.

Western blot with anti-Rhes antibody of lysates of Q7 cells expressing both Rhes and N-terminal mHtt revealed that 20% of the cell content of Rhes was in the insoluble fraction (Fig. 16B).

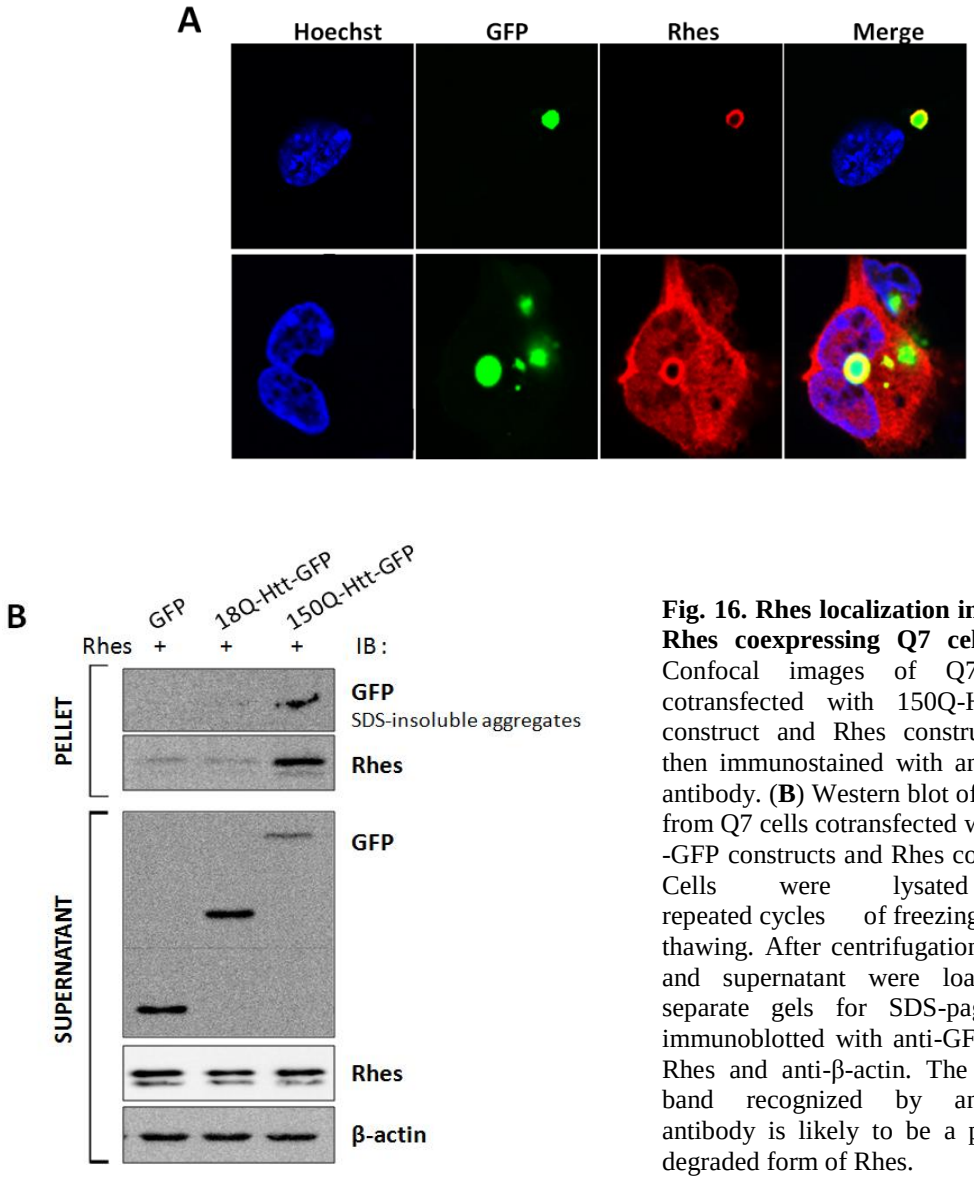

Fig. 16. Rhes localization in mHtt-Rhes coexpressing Q7 cells. (**A**) Confocal images of Q7 cells cotransfected with 150Q-Htt-GFP construct and Rhes construct and then immunostained with anti-Rhes antibody. (**B**) Western blot of lysates from Q7 cells cotransfected with -GFP constructs and Rhes construct. Cells were lysated by repeated cycles of freezing and thawing. After centrifugation, pellet and supernatant were loaded in separate gels for SDS-page and immunoblotted with anti-GFP, anti-Rhes and anti-β-actin. The thinner band recognized by anti-Rhes antibody is likely to be a partially degraded form of Rhes.

Taken together these data suggest that Rhes is partially sequestered by mHtt aggregates. This recruitment does not seem to lower the concentration of soluble Rhes. However, it has to be considered that in Q7 transfected cells Rhes expression is artificially forced by the strong CMV promoter. It would be worth investigating whether soluble Rhes concentration is unchanged in presence of mHtt even in cells where Rhes is endogenously expressed. In fact, it has been hypothesized that Rhes recruitment by mHtt might lead to decrease in free Rhes concentration and that the harmful consequences of Rhes-mHtt coexpression could be due to a Rhes loss-of-function.[132]

5.3.3 Rhes-Htt coexpression reduces mitochondrial membrane potential

The function of mitochondria in Rhes-Htt coexpressing cells was tested by measuring the mitochondrial membrane potential with TMRM probe (Fig. 17).

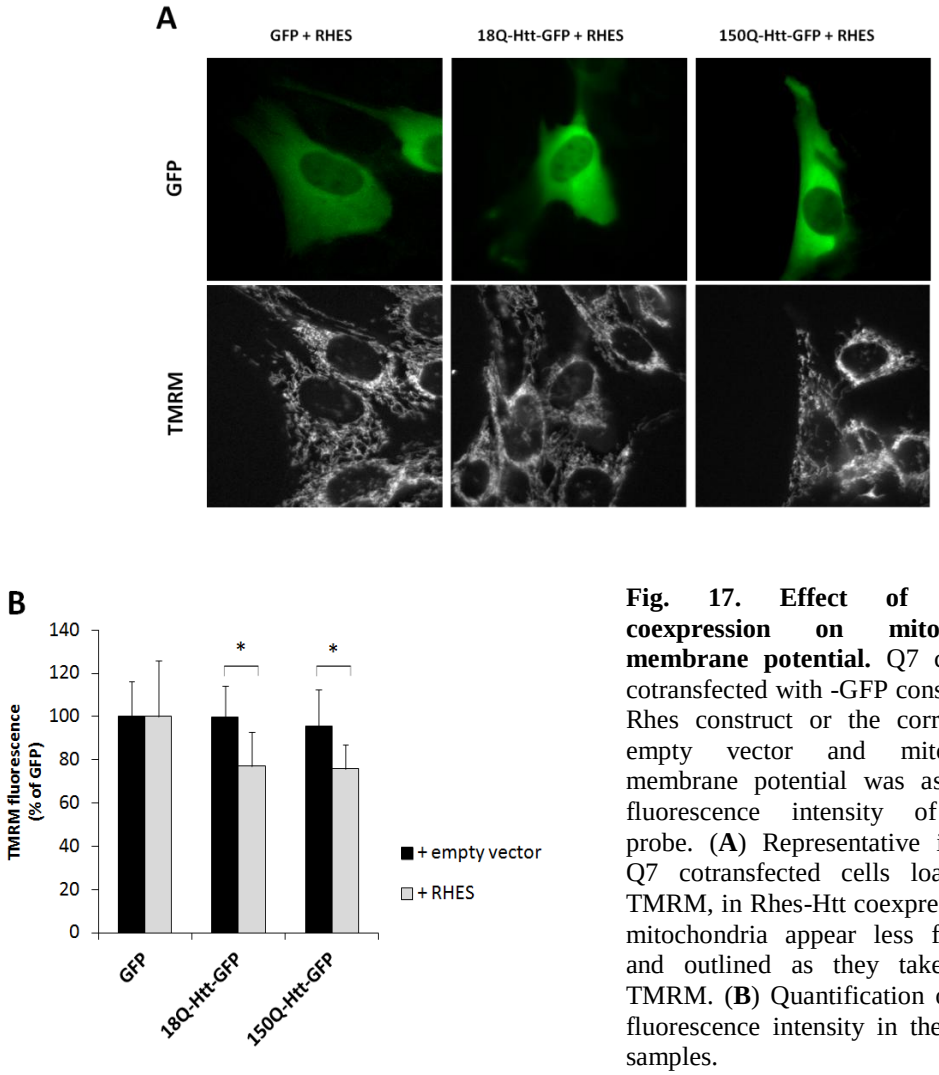

Fig. 17. Effect of Rhes-Htt coexpression on mitochondrial membrane potential. Q7 cells were cotransfected with -GFP constructs and Rhes construct or the corresponding empty vector and mitochondrial membrane potential was assessed as fluorescence intensity of TMRM probe. (**A**) Representative images of Q7 cotransfected cells loaded with TMRM, in Rhes-Htt coexpressing cells mitochondria appear less fluorescent and outlined as they take up less TMRM. (**B**) Quantification of TMRM fluorescence intensity in the analyzed samples.

While Rhes and N-terminal Htt did not affect the mitochondrial membrane potential by themselves, when they were coexpressed a significant decrease in TMRM fluorescence was detected. Assuming that the TMRM distribution across the inner mitochondrial membrane follows ideally the Nernst law, the detected decrease in fluorescence would correspond to a 15 mV loss of potential.

The fact that mHtt expression is associated with mitochondria depolarization only in presence of Rhes suggests that this protein could have a role in determining mitochondrial damage in HD.

5.3.4 Rhes-mHtt coexpression makes cells more sensitive to oxidative stress

An enhanced oxidative stress in HD brains has been described in many reports,[83, 84, 133, 134] but the origin of this increase in ROS has not been identified conclusively. Mitochondria are known to be both a target and a main source of oxidative stress in HD pathogenesis, and being a target can turn into being a source as, for example, respiratory chain defects increase ROS production.[135] We did not observe any increase in ROS following N-terminal mHtt expression in cells lacking Rhes. We wonder whether Rhes could be involved in the oxidative stress associated with mHtt expression

To address this point, we measured ROS level in Q7 cells coexpressing N-terminal mHtt and Rhes by using the DHE probe (Fig. 18A): we failed to detect any significant change. Strikingly, Rhes and mHtt did not increase ROS concentration neither by themselves nor when they were coexpressed. However, if the cell were stressed with H_2O_2, an inducer of oxidative stress, only those expressing both Rhes and mHtt showed a remarkable increase in ROS concentration (Fig. 18B and C).

Thus, these data suggest that Rhes protein could lead to striatal neurodegeneration in HD by making mHtt expressing neurons more sensitive to oxidative stress.

Further investigations are required to understand whether the enhanced susceptibility to oxidative stress is due to an increase in ROS production by defective mitochondria or other sources and oxidative defense mechanisms are involved.

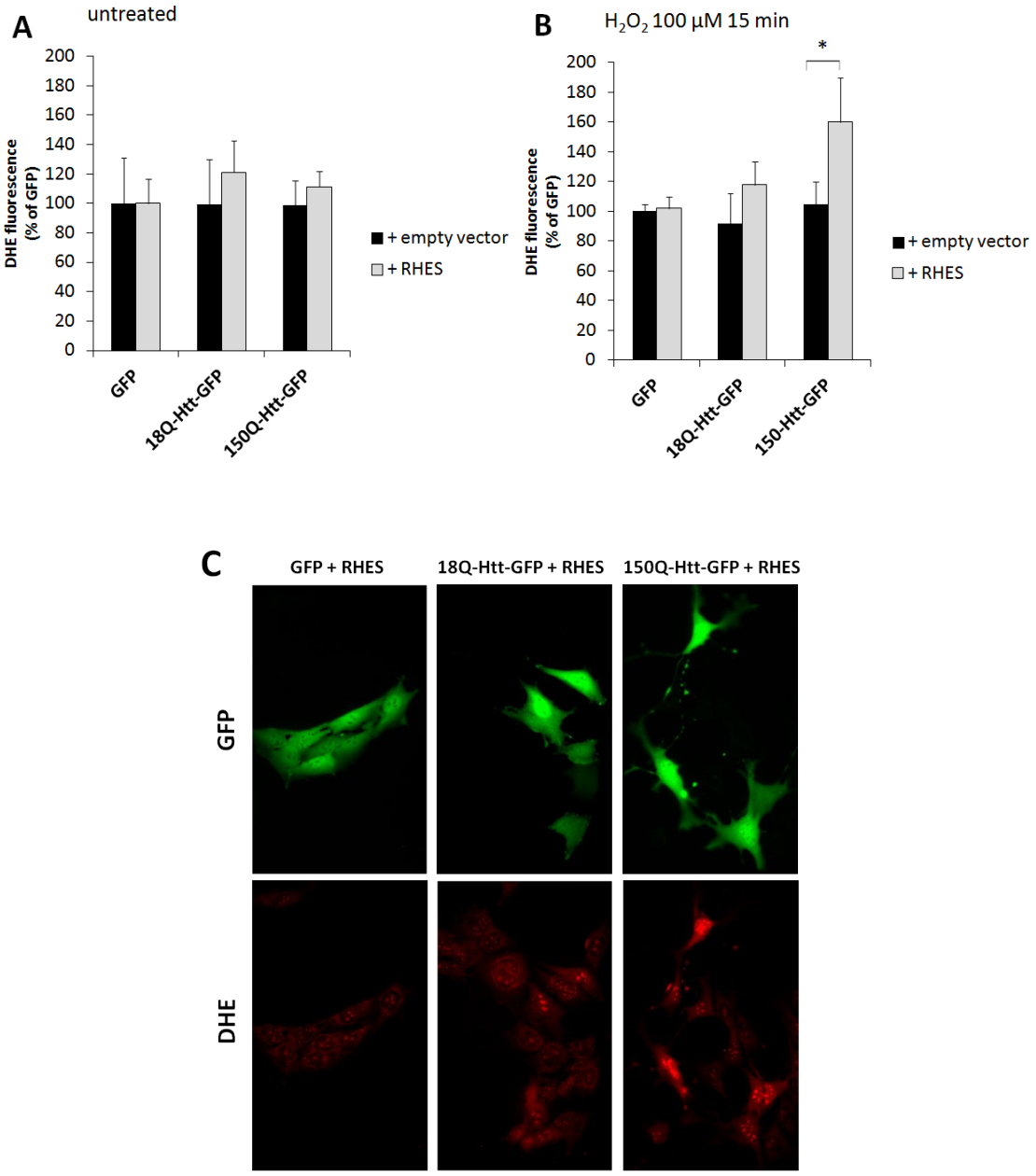

Fig. 18. Effect of Rhes-Htt coexpression on ROS concentration. Q7 cells were cotransfected with –GFP constructs and Rhes construct or the corresponding empty vector and then ROS concentration was assessed as fluorescence intensity of DHE probe. The cells were untreated (**A**) or treated for 15 min with H_2O_2 100 µM before DHE loading (**B**). (**C**) Representative images of Q7 cotransfected cells treated with H_2O_2 and loaded with DHE. Cells that express both Rhes and mHtt show much higher fluorescence.

6. Discussion

Mitochondrial dysfunction is a well documented feature of HD pathogenesis as well as of other neurodegenerative disorders.[125, 136] Several mechanisms have been proposed to explain how mitochondrial defects could activate cell death pathways in HD. However the doubt still remains that these defects represent mere epiphenomena and are not causally linked to neurodegeneration.

The present study provides evidence showing that mitochondrial alteration is not primarily involved in HD pathogenesis and mHtt hardly affects mitochondrial function directly.

In Q111 cells we observed that endogenous expression of mHtt impairs the electron transport chain (ETC) activity, even if this defect is not evident at the steady state. In fact, Q111 and Q7 mitochondria have the same basal respiratory rate and a lower ETC capacity emerges only when maximal respiration is stimulated by FCCP. In addition, a drop in mitochondria membrane potential in Q111 cells is prevented by the compensatory ATP synthase reversal. Thus, the mitochondrial respiratory capacity is actually impaired by mHtt but the cell seems to respond maintaining the normal mitochondrial function. Indeed, Milakovic *et al.* demonstrated that the activities of respiratory complexes are unchanged in Q111 cells and suggested that the defective oxidative phosphorylation could be the result of altered mitochondrial Ca^{2+} concentration.[137]

It has been proposed that mHtt can lower the mitochondrial calcium buffering capacity by favouring permeability transition, with consequent release of cytochrome c and induction of cell death.[71, 126] However, in Q111 isolated mitochondria and permeabilized cells we measured an increased resistance of the permeability transition pore to Ca^{2+}-induced opening in comparison with wild-type counterparts. Importantly, this result was confirmed by mitochondria isolated from both adult and pup HD mice.

These data bring us to exclude that neuronal death in HD is caused by a higher vulnerability of mitochondria to permeability transition. Conversely, it is likely that mitochondria undergo early compensatory changes to become more resistant. It has been previously demonstrated in hepatocyte mitochondria by Klohn *et al*. that

mitochondria are able to adapt to a stressful environment by lowering the sensitivity of the permeability transition pore.[138]

Two plausible stress factors that can trigger this enhanced resistance are Ca^{2+} and ROS. Mitochondria of mHtt expressing cells are known to be exposed to persistently high Ca^{2+} concentration. For example, it is reported that mHtt and HAP1A form a ternary complex with the $InsP_3$ receptor, potentiating its Ca^{2+}-releasing activity.[62] Moreover, NMDA receptors are subject to excitotoxicity[58] that provokes an increase in cytosolic Ca^{2+} concentration. Finally, also the increase in contact sites between endoplasmic reticulum and mitochondria observed in Q111 cells is a likely stress factor (*unpublished preliminary data* from Giacomello M., Scorrano's group, University of Padua), since it could result in enhanced Ca^{2+} transfer between the two organelles and induction of apoptosis.

As far as oxidative stress is concerned, previous studies showed that in Q111 cells ROS concentration does not differ from the control.[126] Therefore oxidative stress is not likely to be involved in the adaptive response of Q111 mitochondria.

Similarly to what we have seen in Q111 cells, also the transient expression of the N-terminal fragment of mHtt seems not to associate with a major mitochondrial damage.

Expression of N-terminal mHtt in animal models reproduce a severe phenotype of HD[130] and when we overexpressed N-terminal mHtt in Q7 and HEK293 cells, we indeed measured a significant increase in cell death. However, this does not correlate with mitochondrial alteration in terms of membrane potential or ROS concentration.

Thus, we can hypothesize that the mitochondrial derangement detected in HD patients and models is not on top of the cascade of events leading neurodegeneration, although, as in any given disease, mitochondrial dysfunction can become apparent at later stages. On the other hand, it is possible that in some circumstances mitochondria sense and amplify alterations that occur elsewhere in the cell. For example, mHtt accumulation compromises autophagic clearance and this can result in delayed engulfment of defective mitochondria.[63] Alternatively, Ca^{2+} dyshomeostasis induced by mHtt can affect mitochondria by means of abnormal regulation of Ca^{2+}-dependent enzymes, Ca^{2+}-overload or increased fragmentation.[95] Mutant Htt represses transcription of several nuclear genes and some of them are relevant for mitochondria function, such as PGC-1α[54] and CREB-dependent OXPHOS proteins.[55] Therefore, as a late process, mitochondrial defects can be secondary to impaired nuclear transcription.

The present data suggest that mHtt *per se* does not affect mitochondria as a primary effect, but it is still possible that other factors are involved. Here we showed that the striatal protein Rhes can play a role in provoking mitochondrial damage in HD.

As already seen by Subramaniam *et al.*, and here confirmed in our model, Rhes decreases mHtt aggregation and increases its cytotoxicity.[116] So, in accordance with the current view,[139] large mHtt inclusions seem not to harm the cell. The mechanisms underlying the Rhes toxic effect has not been understood yet. Interestingly, here we demonstrated that the coexpression of Rhes and N-terminal mHtt causes a loss of mitochondrial membrane potential, whereas the expression of one of the two proteins does not have any effect. Moreover, Rhes-mHtt copresence makes cells highly susceptible to oxidative stress. These two detrimental consequences of mHtt-Rhes coexpression could contribute markedly to neuronal death in the striatum and Rhes can be, at least partially, responsible for the striatal specificity of HD neurodegeneration.

In several cell models, Rhes proved to SUMOylate mHtt at its N-terminus.[116, 140] This modification can potentially alter protein-protein interactions in which mHtt is involved or create new ones with negative effects on cell function. SUMOylation of mHtt is known to reduce the presence of large SDS-insoluble aggregates and this could results in a rise of small oligomeric forms that many studies indentified as the most dangerous species.[49] Additionally, it would be worth examining the transcriptional effect of mHtt in presence of Rhes. SUMOylation potentiates the ability of mHtt to repress transcription.[43] Mutant Htt N-terminus includes a cytoplasmic retention signal such that, once removed, mHtt accumulates in the nucleus. [141] Thus it is tempting to think that the Rhes-mediated SUMOylation of mHtt masks this cytoplasmic retention signal allowing easier entry into the nucleus where mHtt represses transcription with lethal consequences on mitochondria function and cell viability. Preliminary data (*not shown*) from Q7 transfected cells actually showed that, in presence of Rhes, a higher percentage of N-terminal mHtt localizes in the nucleus.

The first candidate to be involved in transcription-dependent mitochondrial defects would be PGC-1α. This is a co-activator of transcription that regulates a number of cellular processes, among them mitochondrial biogenesis, oxidative phosphorylation and the response of mitochondria to oxidative stress by controlling the transcription of ROS-scavenging enzymes. PGC-1α is downregulated in the striatum of HD patients as well as in Q111 cells.[54]

Further experiments will be aimed at clarifying how Rhes interplay with mHtt can cause mitochondrial dysfunction and increased susceptibility to oxidative stress. A more defined knowledge of these pathways and the physiological function of Rhes could help to make it a feasible pharmacological target for HD therapy with the attractive advantage of a selective localization in the brain region affected by the disease.

7. Conclusions

The data presented in this study suggest that mHtt *per se* does not affect mitochondria function as a primary effect and that the mitochondria derangement associated with mHtt expression is not the primary cause of cell death in HD.

We observed that transient expression of N-terminal mHtt in two different cell lines induces an increase in cytotoxicity that does not correlate with mitochondrial impairment. Moreover, mitochondria isolated from HD mice or from immortalized striatal precursors expressing mHtt are even less prone to undergo permeability transition, presumably as an adaptive change to cope with mHtt-related stress. Therefore, although eventually neuronal death can be caused by the cell death cascade that follows permeability transition pore opening, the present results obtained in neuronal cells do not provide any evidence that mHtt expression affects directly mitochondrial function. We also showed that, even though mHtt alters the electron transport chain activity, immortalized striatal cells are able to maintain the basal respiratory rate and the proton gradient across the inner mitochondrial membrane which are essential to allow proper mitochondrial function.

These findings lead us to hypothesize that in HD the loss of mitochondrial function follows the alteration of other key cellular process, like, for example, Ca^{2+} homeostasis, transcription and clearance systems. Mitochondrial impairment is likely to be a common feature of dying neurons and this would explain why several neurodegenerative disorders that differ in aetiology and clinical phenotype share similar mitochondrial alterations. Remarkably, in HD patients these alterations were documented mainly in *post mortem* samples which are very little indicative of the actual trigger of HD pathogenesis.

In the second part of this study we characterized the striatal protein Rhes as a relevant contributor to mitochondrial damage in HD and we provided new insights into the mechanism that underlies the mHtt-Rhes interplay. In fact, we demonstrated that the coexpression of mHtt and Rhes leads to increased susceptibility to oxidative stress and loss of mitochondrial membrane potential.

To characterize the pathways whereby mHtt can affect mitochondrial function in the striatum and to understand how this alteration is framed in the sequence of events

leading to neuronal death are crucial points to identify new potential therapeutic targets to modulate HD progression.

Additional studies, addressing mitochondrial function in HD neurons that endogenously express Rhes will be of importance to elucidate the disorder pathogenesis.

8. References

1. Myers, R.H. *et al.* De novo expansion of a (CAG)n repeat in sporadic Huntington's disease. *Nature genetics* **5**, 168-173 (1993).
2. Myers, R.H. *et al.* Clinical and neuropathologic assessment of severity in Huntington's disease. *Neurology* **38**, 341-347 (1988).
3. Rubinsztein, D.C. *et al.* Phenotypic characterization of individuals with 30-40 CAG repeats in the Huntington disease (HD) gene reveals HD cases with 36 repeats and apparently normal elderly individuals with 36-39 repeats. *American journal of human genetics* **59**, 16-22 (1996).
4. Wexler, N.S. *et al.* Venezuelan kindreds reveal that genetic and environmental factors modulate Huntington's disease age of onset. *Proceedings of the National Academy of Sciences of the United States of America* **101**, 3498-3503 (2004).
5. Rosenblatt, A. *et al.* The association of CAG repeat length with clinical progression in Huntington disease. *Neurology* **66**, 1016-1020 (2006).
6. Sieradzan, K.A. & Mann, D.M. The selective vulnerability of nerve cells in Huntington's disease. *Neuropathology and applied neurobiology* **27**, 1-21 (2001).
7. Vonsattel, J.P. *et al.* Neuropathological classification of Huntington's disease. *Journal of neuropathology and experimental neurology* **44**, 559-577 (1985).
8. Vonsattel, J.P. & DiFiglia, M. Huntington disease. *Journal of neuropathology and experimental neurology* **57**, 369-384 (1998).
9. Kassubek, J. *et al.* Topography of cerebral atrophy in early Huntington's disease: a voxel based morphometric MRI study. *Journal of neurology, neurosurgery, and psychiatry* **75**, 213-220 (2004).
10. Walker, F.O. Huntington's disease. *Lancet* **369**, 218-228 (2007).
11. Politis, M. *et al.* Hypothalamic involvement in Huntington's disease: an in vivo PET study. *Brain : a journal of neurology* **131**, 2860-2869 (2008).
12. Marder, K. *et al.* Rate of functional decline in Huntington's disease. Huntington Study Group. *Neurology* **54**, 452-458 (2000).
13. Rosenblatt, A. Neuropsychiatry of Huntington's disease. *Dialogues in clinical neuroscience* **9**, 191-197 (2007).
14. Shao, J. & Diamond, M.I. Polyglutamine diseases: emerging concepts in pathogenesis and therapy. *Human molecular genetics* **16 Spec No. 2**, R115-123 (2007).
15. DiFiglia, M. *et al.* Huntingtin is a cytoplasmic protein associated with vesicles in human and rat brain neurons. *Neuron* **14**, 1075-1081 (1995).
16. Trottier, Y. *et al.* Cellular localization of the Huntington's disease protein and discrimination of the normal and mutated form. *Nature genetics* **10**, 104-110 (1995).
17. Fusco, F.R. *et al.* Cellular localization of huntingtin in striatal and cortical neurons in rats: lack of correlation with neuronal vulnerability in Huntington's disease. *The Journal of neuroscience : the official journal of the Society for Neuroscience* **19**, 1189-1202 (1999).
18. Hilditch-Maguire, P. *et al.* Huntingtin: an iron-regulated protein essential for normal nuclear and perinuclear organelles. *Human molecular genetics* **9**, 2789-2797 (2000).
19. Hoffner, G., Kahlem, P. & Djian, P. Perinuclear localization of huntingtin as a consequence of its binding to microtubules through an interaction with beta-tubulin: relevance to Huntington's disease. *Journal of cell science* **115**, 941-948 (2002).
20. Velier, J. *et al.* Wild-type and mutant huntingtins function in vesicle trafficking in the secretory and endocytic pathways. *Experimental neurology* **152**, 34-40 (1998).

21. Andrade, M.A. & Bork, P. HEAT repeats in the Huntington's disease protein. *Nature genetics* **11**, 115-116 (1995).
22. Li, S.H. & Li, X.J. Huntingtin-protein interactions and the pathogenesis of Huntington's disease. *Trends in genetics : TIG* **20**, 146-154 (2004).
23. Sugars, K.L. & Rubinsztein, D.C. Transcriptional abnormalities in Huntington disease. *Trends in genetics : TIG* **19**, 233-238 (2003).
24. Faber, P.W. *et al.* Huntingtin interacts with a family of WW domain proteins. *Human molecular genetics* **7**, 1463-1474 (1998).
25. Zuccato, C. *et al.* Huntingtin interacts with REST/NRSF to modulate the transcription of NRSE-controlled neuronal genes. *Nature genetics* **35**, 76-83 (2003).
26. Zuccato, C. & Cattaneo, E. Role of brain-derived neurotrophic factor in Huntington's disease. *Progress in neurobiology* **81**, 294-330 (2007).
27. Li, X.J. *et al.* A huntingtin-associated protein enriched in brain with implications for pathology. *Nature* **378**, 398-402 (1995).
28. Kalchman, M.A. *et al.* HIP1, a human homologue of S. cerevisiae Sla2p, interacts with membrane-associated huntingtin in the brain. *Nature genetics* **16**, 44-53 (1997).
29. McGuire, J.R., Rong, J., Li, S.H. & Li, X.J. Interaction of Huntingtin-associated protein-1 with kinesin light chain: implications in intracellular trafficking in neurons. *The Journal of biological chemistry* **281**, 3552-3559 (2006).
30. Li, S.H., Gutekunst, C.A., Hersch, S.M. & Li, X.J. Interaction of huntingtin-associated protein with dynactin P150Glued. *The Journal of neuroscience : the official journal of the Society for Neuroscience* **18**, 1261-1269 (1998).
31. Gauthier, L.R. *et al.* Huntingtin controls neurotrophic support and survival of neurons by enhancing BDNF vesicular transport along microtubules. *Cell* **118**, 127-138 (2004).
32. Gervais, F.G. *et al.* Recruitment and activation of caspase-8 by the Huntingtin-interacting protein Hip-1 and a novel partner Hippi. *Nature cell biology* **4**, 95-105 (2002).
33. Rigamonti, D. *et al.* Wild-type huntingtin protects from apoptosis upstream of caspase-3. *The Journal of neuroscience : the official journal of the Society for Neuroscience* **20**, 3705-3713 (2000).
34. Rigamonti, D. *et al.* Huntingtin's neuroprotective activity occurs via inhibition of procaspase-9 processing. *The Journal of biological chemistry* **276**, 14545-14548 (2001).
35. Nasir, J. *et al.* Targeted disruption of the Huntington's disease gene results in embryonic lethality and behavioral and morphological changes in heterozygotes. *Cell* **81**, 811-823 (1995).
36. Dragatsis, I., Levine, M.S. & Zeitlin, S. Inactivation of Hdh in the brain and testis results in progressive neurodegeneration and sterility in mice. *Nature genetics* **26**, 300-306 (2000).
37. Cattaneo, E. *et al.* Loss of normal huntingtin function: new developments in Huntington's disease research. *Trends in neurosciences* **24**, 182-188 (2001).
38. Wellington, C.L. *et al.* Caspase cleavage of mutant huntingtin precedes neurodegeneration in Huntington's disease. *The Journal of neuroscience : the official journal of the Society for Neuroscience* **22**, 7862-7872 (2002).
39. Kim, Y.J. *et al.* Caspase 3-cleaved N-terminal fragments of wild-type and mutant huntingtin are present in normal and Huntington's disease brains, associate with membranes, and undergo calpain-dependent proteolysis. *Proceedings of the National Academy of Sciences of the United States of America* **98**, 12784-12789 (2001).
40. Kalchman, M.A. *et al.* Huntingtin is ubiquitinated and interacts with a specific ubiquitin-conjugating enzyme. *The Journal of biological chemistry* **271**, 19385-19394 (1996).
41. Luo, S., Vacher, C., Davies, J.E. & Rubinsztein, D.C. Cdk5 phosphorylation of huntingtin reduces its cleavage by caspases: implications for mutant huntingtin toxicity. *The Journal of cell biology* **169**, 647-656 (2005).

42. Thompson, L.M. *et al.* IKK phosphorylates Huntingtin and targets it for degradation by the proteasome and lysosome. *The Journal of cell biology* **187**, 1083-1099 (2009).
43. Steffan, J.S. *et al.* SUMO modification of Huntingtin and Huntington's disease pathology. *Science* **304**, 100-104 (2004).
44. Geiss-Friedlander, R. & Melchior, F. Concepts in sumoylation: a decade on. *Nature reviews. Molecular cell biology* **8**, 947-956 (2007).
45. Yanai, A. *et al.* Palmitoylation of huntingtin by HIP14 is essential for its trafficking and function. *Nature neuroscience* **9**, 824-831 (2006).
46. Jeong, H. *et al.* Acetylation targets mutant huntingtin to autophagosomes for degradation. *Cell* **137**, 60-72 (2009).
47. Bates, G. Huntingtin aggregation and toxicity in Huntington's disease. *Lancet* **361**, 1642-1644 (2003).
48. Saudou, F., Finkbeiner, S., Devys, D. & Greenberg, M.E. Huntingtin acts in the nucleus to induce apoptosis but death does not correlate with the formation of intranuclear inclusions. *Cell* **95**, 55-66 (1998).
49. Lotz, G.P. *et al.* Hsp70 and Hsp40 functionally interact with soluble mutant huntingtin oligomers in a classic ATP-dependent reaction cycle. *The Journal of biological chemistry* **285**, 38183-38193 (2010).
50. Graham, R.K. *et al.* Cleavage at the caspase-6 site is required for neuronal dysfunction and degeneration due to mutant huntingtin. *Cell* **125**, 1179-1191 (2006).
51. Carter, R.J. *et al.* Characterization of progressive motor deficits in mice transgenic for the human Huntington's disease mutation. *The Journal of neuroscience : the official journal of the Society for Neuroscience* **19**, 3248-3257 (1999).
52. Hodges, A. *et al.* Regional and cellular gene expression changes in human Huntington's disease brain. *Human molecular genetics* **15**, 965-977 (2006).
53. Sadri-Vakili, G. & Cha, J.H. Mechanisms of disease: Histone modifications in Huntington's disease. *Nature clinical practice. Neurology* **2**, 330-338 (2006).
54. Cui, L. *et al.* Transcriptional repression of PGC-1alpha by mutant huntingtin leads to mitochondrial dysfunction and neurodegeneration. *Cell* **127**, 59-69 (2006).
55. Steffan, J.S. *et al.* The Huntington's disease protein interacts with p53 and CREB-binding protein and represses transcription. *Proceedings of the National Academy of Sciences of the United States of America* **97**, 6763-6768 (2000).
56. Benn, C.L. *et al.* Huntingtin modulates transcription, occupies gene promoters in vivo, and binds directly to DNA in a polyglutamine-dependent manner. *The Journal of neuroscience : the official journal of the Society for Neuroscience* **28**, 10720-10733 (2008).
57. Ferrer, I., Goutan, E., Marin, C., Rey, M.J. & Ribalta, T. Brain-derived neurotrophic factor in Huntington disease. *Brain Res* **866**, 257-261 (2000).
58. Tabrizi, S.J. *et al.* Biochemical abnormalities and excitotoxicity in Huntington's disease brain. *Annals of neurology* **45**, 25-32 (1999).
59. Zeron, M.M. *et al.* Increased sensitivity to N-methyl-D-aspartate receptor-mediated excitotoxicity in a mouse model of Huntington's disease. *Neuron* **33**, 849-860 (2002).
60. Giacomello, M., Oliveros, J.C., Naranjo, J.R. & Carafoli, E. Neuronal Ca(2+) dyshomeostasis in Huntington disease. *Prion* **7**, 76-84 (2013).
61. Giacomello, M., Hudec, R. & Lopreiato, R. Huntington's disease, calcium, and mitochondria. *Biofactors* **37**, 206-218 (2011).
62. Tang, T. Huntingtin and Huntingtin-Associated Protein 1 Influence Neuronal Calcium Signaling Mediated by Inositol-(1,4,5) Triphosphate Receptor Type 1. *Neuron* **39**, 227-239 (2003).
63. Martinez-Vicente, M. *et al.* Cargo recognition failure is responsible for inefficient autophagy in Huntington's disease. *Nature neuroscience* **13**, 567-576 (2010).

64. Renna, M., Jimenez-Sanchez, M., Sarkar, S. & Rubinsztein, D.C. Chemical inducers of autophagy that enhance the clearance of mutant proteins in neurodegenerative diseases. *The Journal of biological chemistry* **285**, 11061-11067 (2010).
65. Li, X.J. & Li, S. Proteasomal dysfunction in aging and Huntington disease. *Neurobiology of disease* **43**, 4-8 (2011).
66. Bennett, E.J. *et al.* Global changes to the ubiquitin system in Huntington's disease. *Nature* **448**, 704-708 (2007).
67. Chang, D.T., Rintoul, G.L., Pandipati, S. & Reynolds, I.J. Mutant huntingtin aggregates impair mitochondrial movement and trafficking in cortical neurons. *Neurobiology of disease* **22**, 388-400 (2006).
68. Gunawardena, S. *et al.* Disruption of axonal transport by loss of huntingtin or expression of pathogenic polyQ proteins in Drosophila. *Neuron* **40**, 25-40 (2003).
69. Damiano, M., Galvan, L., Deglon, N. & Brouillet, E. Mitochondria in Huntington's disease. *Biochim.Biophys.Acta* (2009).
70. Bolanos, J.P., Almeida, A. & Moncada, S. Glycolysis: a bioenergetic or a survival pathway? *Trends in biochemical sciences* **35**, 145-149 (2010).
71. Panov, A.V. *et al.* Early mitochondrial calcium defects in Huntington's disease are a direct effect of polyglutamines. *Nature neuroscience* **5**, 731-736 (2002).
72. Choo, Y.S., Johnson, G.V., MacDonald, M., Detloff, P.J. & Lesort, M. Mutant huntingtin directly increases susceptibility of mitochondria to the calcium-induced permeability transition and cytochrome c release. *Human molecular genetics* **13**, 1407-1420 (2004).
73. Bae, B.I. *et al.* p53 mediates cellular dysfunction and behavioral abnormalities in Huntington's disease. *Neuron* **47**, 29-41 (2005).
74. McGill, J.K. & Beal, M.F. PGC-1alpha, a new therapeutic target in Huntington's disease? *Cell* **127**, 465-468 (2006).
75. Jenkins, B.G., Koroshetz, W.J., Beal, M.F. & Rosen, B.R. Evidence for impairment of energy metabolism in vivo in Huntington's disease using localized 1H NMR spectroscopy. *Neurology* **43**, 2689-2695 (1993).
76. Kuhl, D.E. *et al.* Local cerebral glucose utilization in symptomatic and presymptomatic Huntington's disease. *Research publications - Association for Research in Nervous and Mental Disease* **63**, 199-209 (1985).
77. Feigin, A. *et al.* Metabolic network abnormalities in early Huntington's disease: an [(18)F]FDG PET study. *Journal of nuclear medicine : official publication, Society of Nuclear Medicine* **42**, 1591-1595 (2001).
78. Mochel, F. & Haller, R.G. Energy deficit in Huntington disease: why it matters. *The Journal of clinical investigation* **121**, 493-499 (2011).
79. Moffett, J.R., Ross, B., Arun, P., Madhavarao, C.N. & Namboodiri, A.M. N-Acetylaspartate in the CNS: from neurodiagnostics to neurobiology. *Progress in neurobiology* **81**, 89-131 (2007).
80. Brennan, W.A., Jr., Bird, E.D. & Aprille, J.R. Regional mitochondrial respiratory activity in Huntington's disease brain. *Journal of neurochemistry* **44**, 1948-1950 (1985).
81. Guidetti, P. *et al.* Early degenerative changes in transgenic mice expressing mutant huntingtin involve dendritic abnormalities but no impairment of mitochondrial energy production. *Experimental neurology* **169**, 340-350 (2001).
82. Butterworth, J., Yates, C.M. & Reynolds, G.P. Distribution of phosphate-activated glutaminase, succinic dehydrogenase, pyruvate dehydrogenase and gamma-glutamyl transpeptidase in post-mortem brain from Huntington's disease and agonal cases. *Journal of the neurological sciences* **67**, 161-171 (1985).
83. Browne, S.E. & Beal, M.F. Oxidative damage in Huntington's disease pathogenesis. *Antioxidants & redox signaling* **8**, 2061-2073 (2006).
84. Chen, C.M. *et al.* Increased oxidative damage and mitochondrial abnormalities in the peripheral blood of Huntington's disease patients. *Biochemical and biophysical research communications* **359**, 335-340 (2007).

85. Sorolla, M.A. *et al.* Proteomic and oxidative stress analysis in human brain samples of Huntington disease. *Free radical biology & medicine* **45**, 667-678 (2008).
86. Santamaria, A. *et al.* Comparative analysis of superoxide dismutase activity between acute pharmacological models and a transgenic mouse model of Huntington's disease. *Neurochemical research* **26**, 419-424 (2001).
87. Brouillet, E., Jacquard, C., Bizat, N. & Blum, D. 3-Nitropropionic acid: a mitochondrial toxin to uncover physiopathological mechanisms underlying striatal degeneration in Huntington's disease. *Journal of neurochemistry* **95**, 1521-1540 (2005).
88. Wang, J.Q. *et al.* Dysregulation of mitochondrial calcium signaling and superoxide flashes cause mitochondrial genomic DNA damage in Huntington disease. *The Journal of biological chemistry* **288**, 3070-3084 (2013).
89. Valencia, A. *et al.* Elevated NADPH oxidase activity contributes to oxidative stress and cell death in Huntington's disease. *Human molecular genetics* **22**, 1112-1131 (2013).
90. Brustovetsky, N. *et al.* Age-dependent changes in the calcium sensitivity of striatal mitochondria in mouse models of Huntington's Disease. *Journal of neurochemistry* **93**, 1361-1370 (2005).
91. Oliveira, J.M. *et al.* Mitochondrial dysfunction in Huntington's disease: the bioenergetics of isolated and in situ mitochondria from transgenic mice. *Journal of neurochemistry* **101**, 241-249 (2007).
92. Chalmers, S. & Nicholls, D.G. The relationship between free and total calcium concentrations in the matrix of liver and brain mitochondria. *J.Biol.Chem.* **278**, 19062-19070 (2003).
93. Brown, M.R., Sullivan, P.G. & Geddes, J.W. Synaptic mitochondria are more susceptible to Ca2+overload than nonsynaptic mitochondria. *The Journal of biological chemistry* **281**, 11658-11668 (2006).
94. Oliveira, J.M. *et al.* Mitochondrial-dependent Ca2+ handling in Huntington's disease striatal cells: effect of histone deacetylase inhibitors. *The Journal of neuroscience : the official journal of the Society for Neuroscience* **26**, 11174-11186 (2006).
95. Costa, V. *et al.* Mitochondrial fission and cristae disruption increase the response of cell models of Huntington's disease to apoptotic stimuli. *EMBO molecular medicine* **2**, 490-503 (2010).
96. Jin, Y.N. *et al.* Impaired mitochondrial dynamics and Nrf2 signaling contribute to compromised responses to oxidative stress in striatal cells expressing full-length mutant huntingtin. *PLoS One* **8**, e57932 (2013).
97. Wang, H., Lim, P.J., Karbowski, M. & Monteiro, M.J. Effects of overexpression of huntingtin proteins on mitochondrial integrity. *Human molecular genetics* **18**, 737-752 (2009).
98. Song, W. *et al.* Mutant huntingtin binds the mitochondrial fission GTPase dynamin-related protein-1 and increases its enzymatic activity. *Nature medicine* **17**, 377-382 (2011).
99. Guo, X. *et al.* Inhibition of mitochondrial fragmentation diminishes Huntington's disease-associated neurodegeneration. *The Journal of clinical investigation* **123**, 5371-5388 (2013).
100. Trushina, E. *et al.* Mutant huntingtin impairs axonal trafficking in mammalian neurons in vivo and in vitro. *Mol Cell Biol* **24**, 8195-8209 (2004).
101. Orr, A.L. *et al.* N-terminal mutant huntingtin associates with mitochondria and impairs mitochondrial trafficking. *The Journal of neuroscience : the official journal of the Society for Neuroscience* **28**, 2783-2792 (2008).
102. Oliveira, J.M. & Goncalves, J. In situ mitochondrial Ca2+ buffering differences of intact neurons and astrocytes from cortex and striatum. *The Journal of biological chemistry* **284**, 5010-5020 (2009).

103. Usui, H. *et al.* Isolation of clones of rat striatum-specific mRNAs by directional tag PCR subtraction. *The Journal of neuroscience : the official journal of the Society for Neuroscience* **14**, 4915-4926 (1994).
104. Falk, J.D. *et al.* Rhes: A striatal-specific Ras homolog related to Dexras1. *Journal of neuroscience research* **57**, 782-788 (1999).
105. Chan, S.L., Monks, L.K., Gao, H., Deaville, P. & Morgan, N.G. Identification of the monomeric G-protein, Rhes, as an efaroxan-regulated protein in the pancreatic beta-cell. *British journal of pharmacology* **136**, 31-36 (2002).
106. Spano, D. *et al.* Rhes is involved in striatal function. *Mol Cell Biol* **24**, 5788-5796 (2004).
107. Harrison, L.M., Lahoste, G.J. & Ruskin, D.N. Ontogeny and dopaminergic regulation in brain of Ras homolog enriched in striatum (Rhes). *Brain Res* **1245**, 16-25 (2008).
108. Vargiu, P. *et al.* The small GTP-binding protein, Rhes, regulates signal transduction from G protein-coupled receptors. *Oncogene* **23**, 559-568 (2004).
109. Thapliyal, A., Bannister, R.A., Hanks, C. & Adams, B.A. The monomeric G proteins AGS1 and Rhes selectively influence Galphai-dependent signaling to modulate N-type (CaV2.2) calcium channels. *American journal of physiology. Cell physiology* **295**, C1417-1426 (2008).
110. Errico, F. *et al.* The GTP-binding protein Rhes modulates dopamine signaling in striatal medium spiny neurons. *Molecular and cellular neurosciences* **37**, 335-345 (2008).
111. Subramaniam, S. *et al.* Rhes, a striatal-enriched small G protein, mediates mTOR signaling and L-DOPA-induced dyskinesia. *Nature neuroscience* **15**, 191-193 (2012).
112. Wullschleger, S., Loewith, R. & Hall, M.N. TOR signaling in growth and metabolism. *Cell* **124**, 471-484 (2006).
113. Bang, S., Steenstra, C. & Kim, S.F. Striatum specific protein, Rhes regulates AKT pathway. *Neuroscience letters* **521**, 142-147 (2012).
114. Subramaniam, S. *et al.* Rhes, a physiologic regulator of sumoylation, enhances cross-sumoylation between the basic sumoylation enzymes E1 and Ubc9. *The Journal of biological chemistry* **285**, 20428-20432 (2010).
115. Harrison, L.M. & LaHoste, G.J. Rhes, the Ras homolog enriched in striatum, is reduced under conditions of dopamine supersensitivity. *Neuroscience* **137**, 483-492 (2006).
116. Subramaniam, S., Sixt, K.M., Barrow, R. & Snyder, S.H. Rhes, a striatal specific protein, mediates mutant-huntingtin cytotoxicity. *Science* **324**, 1327-1330 (2009).
117. Seredenina, T., Gokce, O. & Luthi-Carter, R. Decreased striatal RGS2 expression is neuroprotective in Huntington's disease (HD) and exemplifies a compensatory aspect of HD-induced gene regulation. *PLoS One* **6**, e22231 (2011).
118. Mealer, R.G., Subramaniam, S. & Snyder, S.H. Rhes deletion is neuroprotective in the 3-nitropropionic acid model of Huntington's disease. *The Journal of neuroscience : the official journal of the Society for Neuroscience* **33**, 4206-4210 (2013).
119. Baiamonte, B.A., Lee, F.A., Brewer, S.T., Spano, D. & LaHoste, G.J. Attenuation of Rhes activity significantly delays the appearance of behavioral symptoms in a mouse model of Huntington's disease. *PLoS One* **8**, e53606 (2013).
120. Lu, B. & Palacino, J. A novel human embryonic stem cell-derived Huntington's disease neuronal model exhibits mutant huntingtin (mHTT) aggregates and soluble mHTT-dependent neurodegeneration. *FASEB journal : official publication of the Federation of American Societies for Experimental Biology* **27**, 1820-1829 (2013).
121. Sbodio, J.I., Paul, B.D., Machamer, C.E. & Snyder, S.H. Golgi protein ACBD3 mediates neurotoxicity associated with Huntington's disease. *Cell reports* **4**, 890-897 (2013).
122. Okamoto, S. *et al.* Balance between synaptic versus extrasynaptic NMDA receptor activity influences inclusions and neurotoxicity of mutant huntingtin. *Nature medicine* **15**, 1407-1413 (2009).
123. Mealer, R.G., Murray, A.J., Shahani, N., Subramaniam, S. & Snyder, S.H. Rhes, a Striatal-Selective Protein Implicated in Huntington Disease, Binds Beclin-1 and Activates Autophagy. *The Journal of biological chemistry* (2013).

124. Trettel, F. *et al.* Dominant phenotypes produced by the HD mutation in STHdh(Q111) striatal cells. *Human molecular genetics* **9**, 2799-2809 (2000).
125. Oliveira, J.M. Nature and cause of mitochondrial dysfunction in Huntington's disease: focusing on huntingtin and the striatum. *Journal of neurochemistry* **114**, 1-12 (2010).
126. Lim, D. *et al.* Calcium homeostasis and mitochondrial dysfunction in striatal neurons of Huntington disease. *The Journal of biological chemistry* **283**, 5780-5789 (2008).
127. Slow, E.J. Selective striatal neuronal loss in a YAC128 mouse model of Huntington disease. *Human molecular genetics* **12**, 1555-1567 (2003).
128. Oliveira, J.M. Mitochondrial bioenergetics and dynamics in Huntington's disease: tripartite synapses and selective striatal degeneration. *Journal of bioenergetics and biomembranes* **42**, 227-234 (2010).
129. Benchoua, A. *et al.* Involvement of mitochondrial complex II defects in neuronal death produced by N-terminus fragment of mutated huntingtin. *Molecular biology of the cell* **17**, 1652-1663 (2006).
130. Gil, J.M. & Rego, A.C. The R6 lines of transgenic mice: a model for screening new therapies for Huntington's disease. *Brain research reviews* **59**, 410-431 (2009).
131. Davies, S.W. & Scherzinger, E. Nuclear inclusions in Huntington's disease. *Trends in cell biology* **7**, 422 (1997).
132. Subramaniam, S. & Snyder, S.H. Huntington's disease is a disorder of the corpus striatum: focus on Rhes (Ras homologue enriched in the striatum). *Neuropharmacology* **60**, 1187-1192 (2011).
133. Browne, S.E., Ferrante, R.J. & Beal, M.F. Oxidative stress in Huntington's disease. *Brain pathology* **9**, 147-163 (1999).
134. Hersch, S.M. *et al.* Creatine in Huntington disease is safe, tolerable, bioavailable in brain and reduces serum 8OH2'dG. *Neurology* **66**, 250-252 (2006).
135. La Fontaine, M.A., Geddes, J.W., Banks, A. & Butterfield, D.A. 3-nitropropionic acid induced in vivo protein oxidation in striatal and cortical synaptosomes: insights into Huntington's disease. *Brain Res* **858**, 356-362 (2000).
136. Costa, V. & Scorrano, L. Shaping the role of mitochondria in the pathogenesis of Huntington's disease. *The EMBO journal* **31**, 1853-1864 (2012).
137. Milakovic, T. & Johnson, G.V. Mitochondrial respiration and ATP production are significantly impaired in striatal cells expressing mutant huntingtin. *The Journal of biological chemistry* **280**, 30773-30782 (2005).
138. Klohn, P.C. *et al.* Early resistance to cell death and to onset of the mitochondrial permeability transition during hepatocarcinogenesis with 2-acetylaminofluorene. *Proceedings of the National Academy of Sciences of the United States of America* **100**, 10014-10019 (2003).
139. Arrasate, M., Mitra, S., Schweitzer, E.S., Segal, M.R. & Finkbeiner, S. Inclusion body formation reduces levels of mutant huntingtin and the risk of neuronal death. *Nature* **431**, 805-810 (2004).
140. O'Rourke, J.G. *et al.* SUMO-2 and PIAS1 modulate insoluble mutant huntingtin protein accumulation. *Cell reports* **4**, 362-375 (2013).
141. Rockabrand, E. *et al.* The first 17 amino acids of Huntingtin modulate its sub-cellular localization, aggregation and effects on calcium homeostasis. *Human molecular genetics* **16**, 61-77 (2007).

Acknowledgements

I thank my supervisor Fabio Di Lisa for his great helpfulness. I thank Raffaele Lopreiato for providing plasmids, Marta Giacomello for YAC128 mice and Roman Hudec for STHdh$^{Q7/\ Q7}$ and STHdh$^{Q111/\ Q111}$ cells. I thank all of them and Ernesto Carafoli for the useful suggestions they gave me during my PhD. Thank also to my laboratory colleagues for their everyday support.